UC Irvine
UC Irvine Previously Published Works

Title

NMHCs and halocarbons in Asian continental outflow during the Transport and Chemical Evolution over the Pacific (TRACE-P) Field Campaign: Comparison With PEM-West B

Permalink

https://escholarship.org/uc/item/3cs6n6q8

Journal

Journal of Geophysical Research, 108(D20)

ISSN

0148-0227

Authors

Blake, Nicola J
Blake, Donald R
Simpson, Isobel J
et al.

Publication Date

2003

DOI

10.1029/2002jd003367

Copyright Information

Peer reviewed

NMHCs and halocarbons in Asian continental outflow during the Transport and Chemical Evolution over the Pacific (TRACE-P) Field Campaign: Comparison With PEM-West B

Nicola J. Blake,[1] Donald R. Blake,[1] Isobel J. Simpson,[1] Simone Meinardi,[1]
Aaron L. Swanson,[1] Jimena P. Lopez,[1,2] Aaron S. Katzenstein,[1] Barbara Barletta,[1]
Tomoko Shirai,[3] Elliot Atlas,[4] Glen Sachse,[5] Melody Avery,[5] Stephanie Vay,[5]
Henry E. Fuelberg,[6] Christopher M. Kiley,[6] Kazuyuki Kita,[7] and F. Sherwood Rowland[1]

[1]   We present an overview of the spatial distributions of nonmethane hydrocarbons (NMHCs) and halocarbons observed over the western north Pacific as part of the NASA GTE Transport and Chemical Evolution over the Pacific (TRACE-P) airborne field campaign (February–April 2001). The TRACE-P data are compared with earlier measurements from the Pacific Rim during the Pacific Exploratory Mission-West B (PEM-West B), which took place in February–March 1994, and with emission inventory data for 2000. Despite the limited spatial and temporal data coverage inherent to airborne sampling, mean levels of the longer-lived NMHCs (including ethane, ethyne, and benzene) were remarkably similar to our results during the PEM-West B campaign. By comparison, mixing ratios of the fire extinguisher Halon-1211 (CF_2ClBr) increased by about 50% in the period between 1994 and 2001. Southern China (south of 35°N), and particularly the Shanghai region, appears to have been a substantial source of Halon-1211 during TRACE-P. Our previous analysis of the PEM-West B data employed methyl chloroform (CH_3CCl_3) as a useful industrial tracer. However, regulations have reduced its emissions to the extent that its mixing ratio during TRACE-P was only one-third of that measured in 1994. Methyl chloroform mixing ratio "hot spots," indicating regions downwind of continuing emissions, included outflow from the vicinity of Shanghai, China, but particularly high emission ratios relative to CO were observed close to Japan and Korea. Tetrachloroethene (C_2Cl_4) levels have also decreased significantly, especially north of 25°N, but this gas still remains a useful indicator of northern industrial emissions. Methyl bromide (CH_3Br) levels were systematically 1–2 pptv lower from 1994 to 2001, in accord with recent reports. However, air masses that had been advected over Japan and/or South Korean port cities typically exhibited elevated levels of CH_3Br. As a consequence, emissions of CH_3Br from Japan and Korea calculated employing CH_3Br/CO ratios and scaled to CO emission inventory estimates, were almost as large as for all of south China (south of 35°N). Total east Asian emissions of CH_3Br and CH_3Cl were estimated to be roughly 4.7 Gg/yr and 167 Gg/yr, respectively, in 2001.   *INDEX TERMS:* 0345 Atmospheric Composition and Structure: Pollution—urban and regional (0305); 0365 Atmospheric Composition and Structure: Troposphere—composition and chemistry; 0368 Atmospheric Composition and Structure: Troposphere—constituent transport and chemistry; *KEYWORDS:* NMHCs, halocarbons, methyl bromide, methyl chloride, Halon-1211

[1]Department of Chemistry, University of California, Irvine, California, USA.

[2]Now at NASA Ames Research Center, Moffett Field, California, USA.

[3]Earth Observation Research Center, National Space Development Agency of Japan, Tokyo, Japan.

[4]National Center for Atmospheric Research, Boulder, Colorado, USA.

[5]NASA Langley Research Center, Hampton, Virginia, USA.

[6]Department of Meteorology, Florida State University, Tallahassee, Florida, USA.

[7]Department of Environmental Sciences, Faculty of Science, Ibaraki University, Japan.

1. Introduction

[2] The Transport and Chemical Evolution over the Pacific (TRACE-P) aircraft experiment was the third time NASA's Global Tropospheric Experiment (GTE) has intensively sampled the North Pacific, focusing on the western Pacific Rim region [*Jacob et al.*, 2003]. TRACE-P deployed two aircraft, the NASA Dryden DC-8 and the NASA Wallops P-3B, based out of Hong Kong and Yokota Air Force Base, near Tokyo, Japan in February–April 2001. These same operational bases were also used during the Pacific Exploratory Mission (PEM) West A (in 1991) and B (in 1994) campaigns. The principal objective of TRACE-P was to characterize the composition of Asian outflow, and assess changes in that composition during transport [*Jacob et al.*, 2003]. By contrast, the PEM West campaigns used the NASA DC-8 (only) in a survey mode, addressing a wide variety of objectives [*Hoell et al.*, 1997].

[3] Halocarbons and nonmethane hydrocarbons (NMHCs) are among the most important classes of trace molecules in the atmosphere. Very long-lived halocarbons are linked to stratospheric ozone (O_3) depletion and greenhouse forcing, while NMHCs directly influence the oxidative capacity of the atmosphere and participate as short-lived tropospheric O_3 precursors. To reduce the influence of anthropogenic ozone-depleting substances, the Montreal Protocol on Substances that deplete the Ozone Layer (Montreal Protocol) was agreed to by various governments in 1987, with several Amendments adopted later. The result of the Montreal Protocol and its Amendments (MPA) has been a measured decrease in the concentration of CFCs (chlorofluorocarbons) [*Engel et al.*, 1998; *Montzka et al.*, 1999; *Anderson et al.*, 2000]. There has been a measured decline in the burden of tropospheric chlorine mainly due to a decrease in the atmospheric concentration of methyl chloroform (CH_3CCl_3), which peaked in mid-1992 and has since been decreasing [*Montzka et al.*, 1999; *Anderson et al.*, 2000]. However, atmospheric bromine from industrial halons is still increasing, albeit at a slower rate than was occurring previously [*World Meteorological Organization* (*WMO*), 2002].

[4] Halocarbons with lifetimes much longer than the $1-2$ year interhemispheric mixing time are generally well mixed throughout the troposphere in both hemispheres, with the exception of samples collected close to source regions. We have found evidence for Asian sources of regulated gases such as Halon-1211 (CF_2ClBr), in addition to HCFC-141b and HCFC-22, all of which were enhanced in Asian outflow [*Blake et al.*, 2001], and the sum of organic bromine from methyl bromide (CH_3Br) and halons has more than doubled since the mid-1900s [*WMO*, 2002]. The highly developed industrial regions of Japan, Europe, and North America have ceased production of Halon-1211 and recovery and recycle programs have been effective in reducing total halon emissions from these countries by over 40% since 1992 [*United Nations Environment Programme* (*UNEP*), 1998a]. Despite this success, there has been continuing significant production and use of Halon-1211 by developing countries. Under the Montreal Protocol these countries (termed "Article 5(1) countries") have been given an extra 10 years to phase out halon production and consumption. China is now one of the very few countries that still produces halons [*UNEP*, 2002]

[5] The distribution patterns of NMHCs, halocarbons, and carbon monoxide (CO) can be used to characterize anthropogenic sources such as incomplete combustion and industrial activity. For example, incomplete combustion, including urban fossil fuel and biomass burning, is the principal global source of ethane, ethyne, and CO [*Seinfeld and Pandis*, 1998]. NMHCs are also emitted from liquefied petroleum gas leakage, oil drilling and natural gas fields [*Blake et al.*, 1992; *Blake and Rowland*, 1995]. Tetrachloroethene (C_2Cl_4) is an industrial solvent and chemical intermediate. HCFC-141b is a CFC substitute whose usage is increasing rapidly [*Shirai and Makide*, 1998; *Montzka et al.*, 1999]. Methyl Chloride (CH_3Cl) is a biomass combustion (and wood fuel burning) tracer [e.g., *Rasmussen et al.*, 1980, 1982; *N. J. Blake et al.*, 1996]. Sources of CH_3Cl and CH_3Br are not completely characterized and a substantial imbalance remains in estimates of source and sink magnitudes for both gases; known sinks outweigh known sources for both of these gases [*Butler*, 2000; *WMO*, 2002].

[6] Ethyne is an excellent tracer for long-range pollution transport because it is a general product of incomplete combustion, with major sources from vehicles, biofuels, and biomass burning [*Streets et al.*, 2003]. It has a lifetime of several weeks, which is sufficiently long to track pollution plumes across the Pacific but sufficiently short to provide strong pollution enhancements in these plumes relative to background.

[7] Surface measurements of the concentrations of selected halocarbons and light hydrocarbons are reported by, e.g., *Blake and Rowland* [1995], *Butler et al.* [1998], *Gupta et al.* [1998]; *Montzka et al.* [1999]; and *Prinn et al.* [2000]. However, vertical distribution information is relatively scarce.

[8] For TRACE-P, the University of California, Irvine (UCI) group collected 5483 whole air samples aboard both the NASA DC-8 and the P-3B aircraft during 38 science flights over the western and central Pacific Ocean, from 24 February–10 April 2001. These samples were analyzed at our UCI laboratory for a wide variety of trace gases as described below. Results for selected NMHCs and halocarbons are reported here.

2. Experiment

[9] Individual whole air samples were collected in 2-L stainless steel canisters each equipped with a stainless steel bellows valve. Prior to the mission the canisters were conditioned, evacuated, and 10 Torr of degassed distilled water was added to each canister to quench active surface sites. Canisters were pressurized with air employing a metal bellows pump roughly every $3-7$ min during horizontal flight legs and every $1-3$ min during ascents and descents between 0.15 and 12 km altitude. Horizontal sampling times were approximately 1 min, corresponding to a sampling distance of about 12 km. Approximately 160 air samples were collected per flight aboard the DC-8, and 140 aboard the P-3B.

[10] After each flight, the filled canisters were transported back to the UCI laboratory. Within ten days of being collected, each air sample was analyzed for more than 50 trace gases including the gases that are the focus of this

paper: light nonmethane hydrocarbons (NMHCs) and halocarbons. In addition, alkyl nitrates, dimethyl sulfide (DMS), carbonyl sulfide (OCS), and carbon disulfide (CS_2) were quantified and will be the focus of other papers [e.g., *Simpson et al.*, 2003; N. Blake et al., Carbonyl sulfide (OCS) and carbon disulfide (CS2): Large-scale distributions and emissions from Asia during TRACE-P, manuscript in preparation, 2003]. The same canisters were re-used during successive TRACE-P flights, and two identical analytical systems (sharing the same standards) were operated simultaneously in order to improve the canister turn-around time. Because it takes a few days for the analytical systems to equilibrate and generate the best precision, they were operated 24 hours a day throughout the mission.

[11] Details of the analytical procedures employed by the UCI laboratory can be found in works by *Sive* [1998], *Blake et al.* [2001], and *Colman et al.* [2001] but are outlined as follows. For each sample 1520 ± 1 cm^3 (STP) of air was preconcentrated in a liquid nitrogen-cooled loop. This sample was warmed ($\sim 80^\circ$C) and directed to five different gas chromatographic column/detector combinations. Electron capture detectors (ECD, sensitive to halocarbons and alkyl nitrates), flame ionization detectors (FID, sensitive to hydrocarbons), and quadrupole mass spectrometer detectors (MSD, for unambiguous compound identification, selected ion monitoring) were employed. The first column-detector combination (abbreviated as "DB5ms/MSD") was a DB-5ms column (J&W; 60 m, 0.25 mm I.D., 0.5 μm film thickness) output to a quadrupole MSD (HP-5973). The second combination ("DB1/FID") was a DB-1 column (J&W; 60 m, 0.32 mm I.D., 1 μm film thickness) output to a FID (HP-6890). The third combination ("PLOT-DB1/FID") was a PLOT column (J&W GS-Alumina; 30 m, 0.53 mm I.D.) connected in series to a DB-1 column (J&W; 5 m, 0.53 mm I.D., 1.5 μm film thickness) and output to an FID. The fourth combination ("Restek1701/ECD") was a RESTEK 1701 column (60 m, 0.25 mm I.D., 0.50 μm film thickness) which was output to an ECD. The fifth combination ("DB5-Restek1701/ECD") was a DB-5 (J&W; 30 m, 0.25 mm I.D., 1 μm film thickness) column connected in series to a RESTEK 1701 column (5 m, 0.25 mm I.D., 0.5 μm film thickness) and output to an ECD. The DB5ms/MS, DB1/FID, PLOT-DB1/FID, Restek1701/ECD, and DB5-Restek1701/ECD combinations received 10.1, 15.1, 60.8, 7.2, and 6.8% of the sample flow, respectively.

[12] Our analytical accuracy ranges from 2 to 20%. The precision of the measurements varies by compound and by mixing ratio. For example, the measurement precision is 1% or 1.5 pptv (whichever is larger) for the alkanes and alkynes, and 3% or 3 pptv (whichever is larger) for the alkenes [*Sive*, 1998]. The precision for C_2Cl_4 at 5 pptv is ± 0.05 pptv [*Colman et al.*, 2001]. The limit of detection (LOD) is 3 pptv for the NMHCs. All reported halogenated gases were present at mixing ratios well above their detection limits at all times.

[13] The preparation of primary halocarbon reference standards employs a static dilution method using three different sections of a glass vacuum line. Pure gas is introduced into the first section of the line and is ultimately diluted to a mixing ratio that most closely matches the concentration of the gas in the atmosphere. The range of these halocarbon standards falls between 0.5 and 600 pptv.

The absolute accuracy of this method for a given compound is tied to a manometer measurement and how well the appropriate volume ratios for the dilution system are known [*Wang*, 1993].

[14] Calibration and checking for stability are ongoing processes. We regularly fill a variety of cylinders and electropolished stainless steel pontoons to high pressure with air from different environments for use as short-term and long-term standards. These new standards are referenced to older certified standards for the whole range of gases that we measure. The various older standards are also compared with each other to determine the stability of each component over time. We take part in occasional interlaboratory comparisons, cross-checking our calibration scheme against absolute standards from other groups for both hydrocarbons and halocarbons. As in the work by *Colman et al.* [2001], periodically we compare our long-lived halocarbon measurements (including Halon-1211, CH_3Br, and CH_3Cl) with the published values of global tropospheric averages and growth rates summarized by the *WMO* [1999, 2002].

[15] NMHC calibrations employ a combination of National Bureau of Standards, Scott Specialty Gases (absolute accuracy estimated to be within $\pm 5\%$), and UCI-made standards. We dilute the Scott standards to the low pptv mixing ratio range with helium. These synthetic standards are used to confirm the mixing ratios of previously calibrated cylinders containing whole air stored at high pressure. Typically, our long-term high-pressure whole-air working standards agree with freshly prepared synthetic standards to better than 1% for the light hydrocarbons (C_2–C_5) and to better than 5% for the C_6–C_{10} hydrocarbons. In addition, we have participated in the National Science Foundation sponsored Nonmethane Hydrocarbon Intercomparison Experiment (NOMHICE) [*Apel et al.*, 1994]. Results from NOMHICE demonstrate that our analytical procedures consistently yield accurate identifications of a wide range of unknown hydrocarbons and produce excellent quantitative results [*Apel et al.*, 1994, 1999; *Sive*, 1998].

[16] Although we go to great lengths to carefully condition and recondition our stainless steel sampling canisters, they are known to be subject to slight alkene growth during whole air storage, to a maximum of about 0.1–0.2 pptv per day [*Sive*, 1998]. During both PEM-West B and TRACE-P the samples were analyzed within 10 days of collection, and often sooner, which limited the size of any artifact to 2 pptv or less. Many alkene measurements were below the detection limit of 3 pptv (see results for ethene in next section).

3. Results and Discussion
3.1. Sample Distributions

[17] Figure 1 shows the region close to the Pacific Rim in which sampling efforts were focused during TRACE-P. Figures 2–4 show that few samples were collected over remote regions of the Northern Pacific. Most sampling over the Central Pacific was done during the transit flights via Hawaii. Sampling during PEM-West B was also concentrated close to the Pacific Rim (Figures 1–4) but fewer samples were collected than during TRACE-P. During PEM-West B samples were also collected further north, to
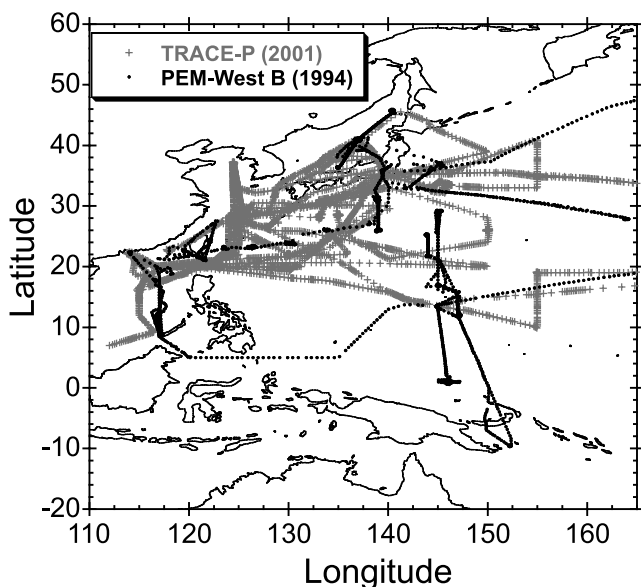
Figure 1. Whole air sample locations for PEM-West B and TRACE-P.

60°N (during transit flights through Anchorage, Alaska) and further south (two sorties reached the equator) (Figures 1–4). The total number of whole air samples that were collected during the dual-aircraft TRACE-P campaign (a total of 5483) far exceeded those collected during the single-aircraft PEM-West B experiment (2041). A similar number (659 versus 777 during TRACE-P and PEM-West B, respectively) were collected at altitudes above 8 km (higher than the flight ceiling of the P-3B), but more than three times as many (3098 versus 888) were collected at mid altitudes (2–8 km) during TRACE-P and more than four times as many (1726 versus 376) were collected below 2 km. The various altitude and latitude/altitude bins used in this paper usually are based on those employed by *Blake et al.* [1997].

3.2. Large-Scale Distributions During TRACE-P

[18] The regional distributions of selected trace gases measured in our whole air samples are illustrated as 2.5° × 2.5° latitude/longitude patches color-coded by average mixing ratio (Figures 2–8). The data are divided into three altitude ranges representing the lower troposphere (0–2 km), middle troposphere (2–8 km) and upper troposphere/lower stratosphere (8–12 km) for ethene, ethyne, CH_3Cl, ethane, CH_3Br, Halon-1211 and C_2Cl_4. The mix of emissions from Asia can be extremely complex [*Kato*, 1996; *Streets et al.*, 2003], and these gases were selected to represent a range of compound lifetimes and source types.

[19] As expected for gases with continental sources, the highest mixing ratios generally are found at low altitudes close to the coast of China and Japan. However, to a first approximation, the rate at which the concentrations decrease
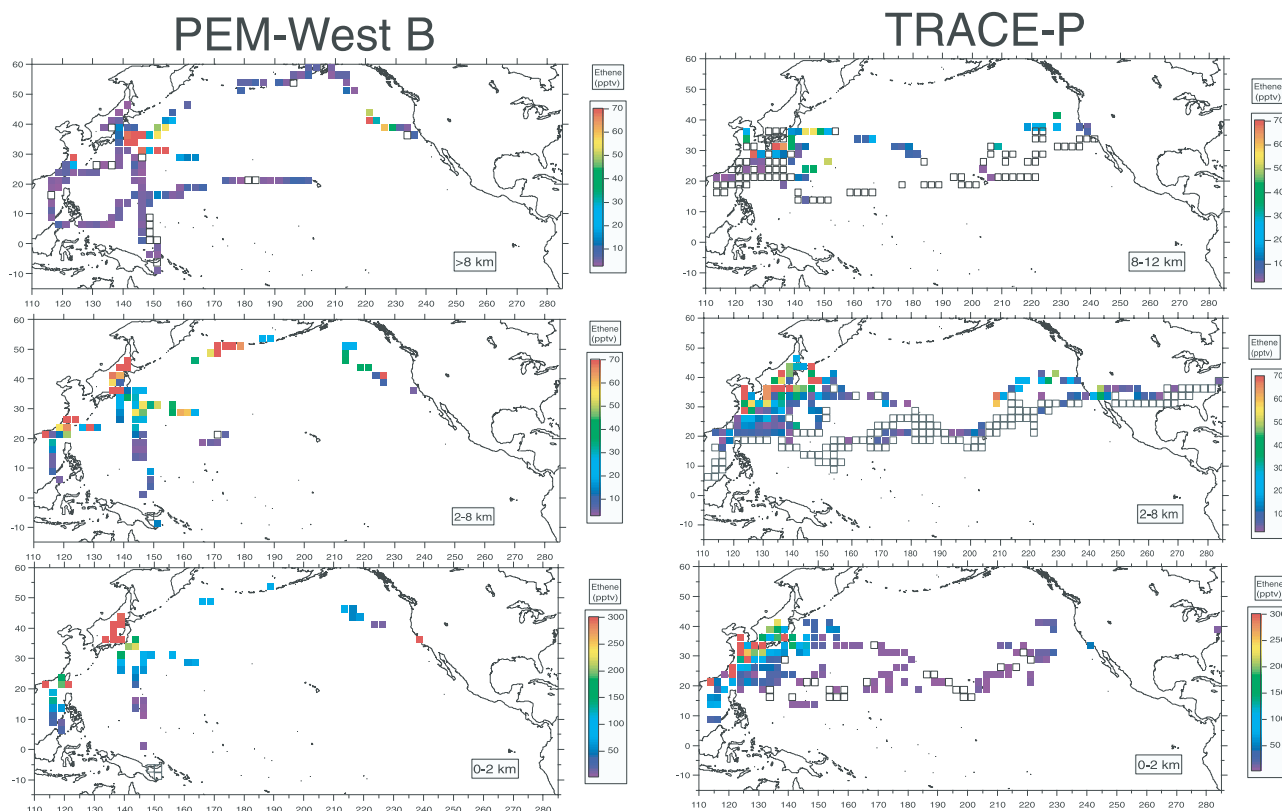
Figure 2. Regional distributions of ethene during PEM-West B and TRACE-P illustrated as 2.5° × 2.5° latitude/longitude patches color-coded by average mixing ratio. Average mixing ratios below detection limit are shown as open squares. The data are divided into three altitude ranges 0–2 km, 2–8 km, and 8–12 km.
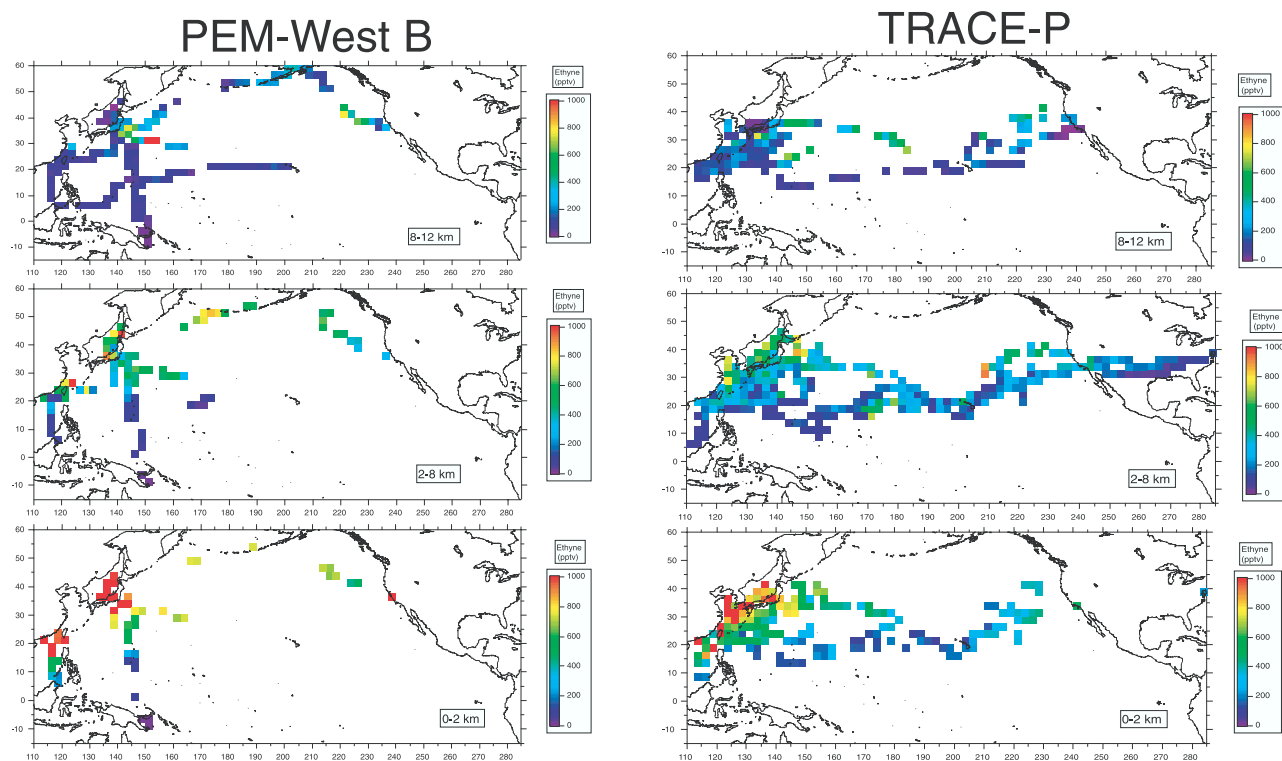
Figure 3. Same as Figure 3 but for ethyne.

as the polluted air masses move away from the continental source regions varies depending on the atmospheric lifetime of each gas. For example, ethene and ethyne have similar, mainly combustion, sources but ethene is relatively short-lived (approximately 2−4 days compared to several weeks for ethyne and ethane). Consequently, mixing ratios of ethene (Figure 2) drop very quickly away from the source regions to very low values, often below detection limit, a
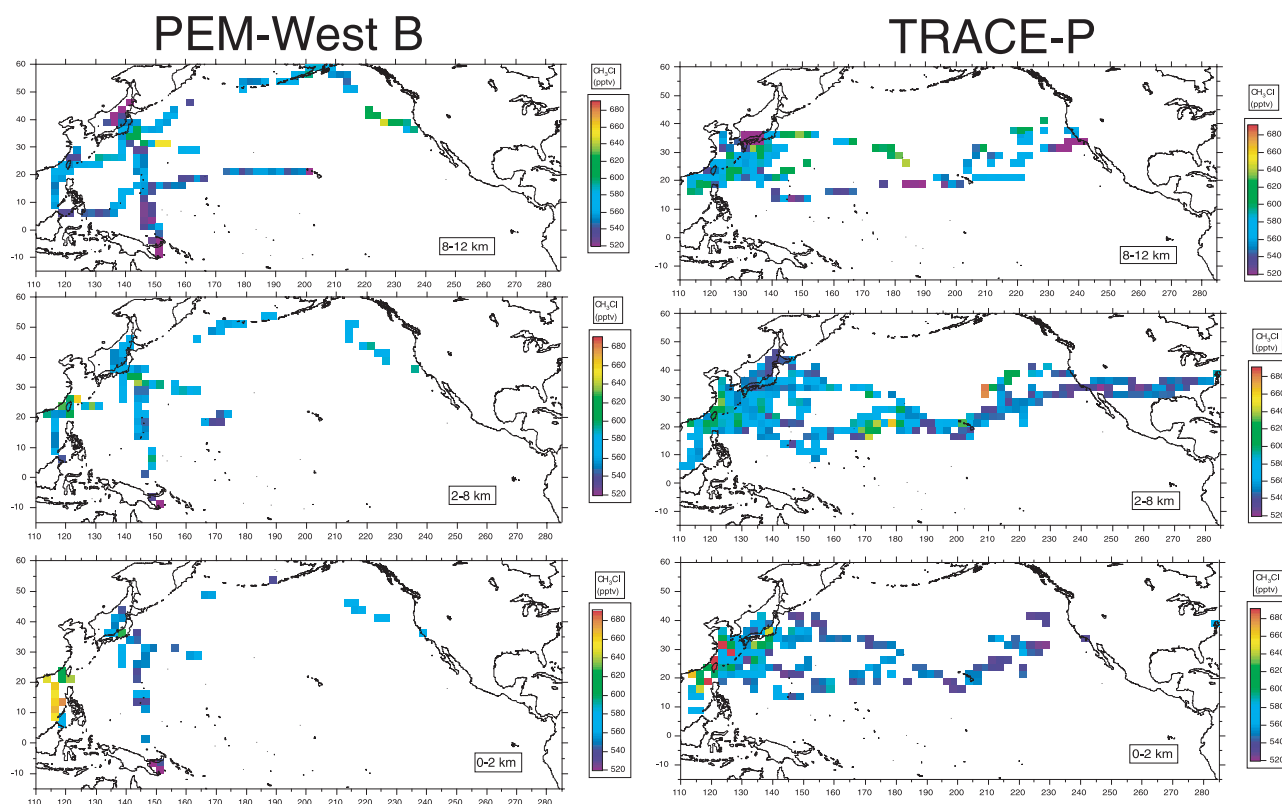
Figure 4. Same as Figure 3 but for CH_3Cl.
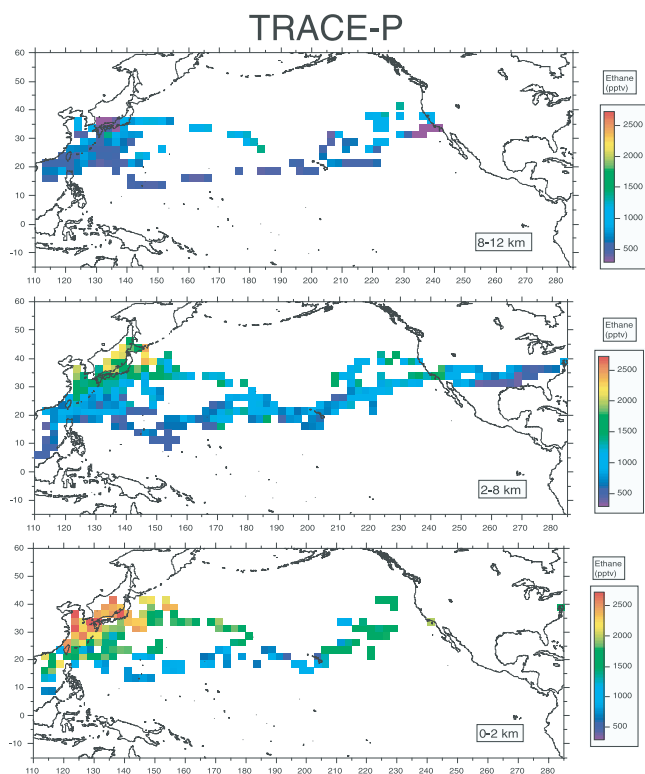
**Figure 5.** Regional distributions of ethane during TRACE-P illustrated as $2.5° \times 2.5°$ latitude/longitude patches color-coded by average mixing ratio. The data are divided into three altitude ranges representing the lower (0–2 km), middle (2–8 km) and upper (8–12 km) troposphere.

few hundred km off shore (Figure 2) compared with the more sustained levels of ethyne and ethane (Figures 3 and 5).

[20] A notable exception to this trend of low ethene mixing ratios over the remote Pacific is a plume of pollution in the mid-troposphere to the NE of the Hawaiian Islands during TRACE-P DC-8 Flight 4, with ethene mixing ratios greater than 50 pptv (Figure 2). This plume also stands out on the large-scale distributions of ethyne (Figure 3) and CH_3Cl (Figure 4). See later for a detailed look at this plume (section 3.5.3).

[21] At the highest altitudes (>8 km), trace gas mixing ratios above Japan and the coast of China are quite low. Relatively high mixing ratios of many trace gases, including ethyne (Figure 3) and Halon-1211 (Figure 7), were found about half way between Japan and Hawaii. By comparison, C_2Cl_4 levels were not notably high in this region (Figure 8). This chemical signature is consistent with the backward trajectories, which suggest air mass origins over the southerly portion of the Asian continent, transported to the Pacific in the prevailing westerly flow [*Fuelberg et al.*, 2003].

[22] At low altitudes (0–2 km) the pattern of CH_3Br enhancements (Figure 6) is unique, with the highest mixing ratios typically near Japan. This is in greatest contrast to the bias towards more southerly enhancements associated with the large-scale distribution of CH_3Cl (Figure 4). The sources of the elevated CH_3Br and CH_3Cl mixing ratios are discussed in sections 3.3.2.5 and 3.3.2.6.

3.3. Comparison of TRACE-P With PEM-West B
3.3.1. Nonmethane Hydrocarbons
[23] The "patch plot" comparisons for ethene, ethyne and CH_3Cl in Figures 2 to 4 show reasonably similar spatial distributions of these three gases during PEM-West B and TRACE-P. The vertical distributions of these and other trace gases for two latitude regions (we chose >25°N and <25°N to be consistent with *Blake et al.* [1997]) are compared for 1-km altitude increments (Figure 9).

[24] NMHC mixing ratios generally were enhanced by at least a factor of two in samples collected below 6 km altitude in Asian outflow, compared with samples collected at higher altitudes, indicating that mean mixing ratios of NMHCs (and most halocarbons) were dominated by anthropogenic sources during both campaigns.

[25] The updated emission inventory data of *Streets et al.* [2003] predicts an increase over the period between the two missions of as much as 10–15 % for total NMHCs. Despite the limited spatial and temporal data coverage inherent to airborne sampling, mean levels of the longer-lived NMHCs (including ethane and ethyne) were remarkably similar to our results during the PEM-West B campaign (Figure 9 and Table 1). In fact, average mixing ratios of several of the shorter-lived NMHCs are significantly lower at latitudes north of 25°N for TRACE-P compared to PEM-West B.

[26] There are several factors that may contribute to the apparent long-term decrease observed, including sampling bias and seasonal change. The series of flights conducted during TRACE-P (and PEM-West B) were designed to meet a variety of objectives, only one of which was a regional characterization [*Jacob et al.*, 2003]. Therefore one of the primary concerns regarding this relatively brief "snapshot" of intensive trace gas sampling over such a large area is
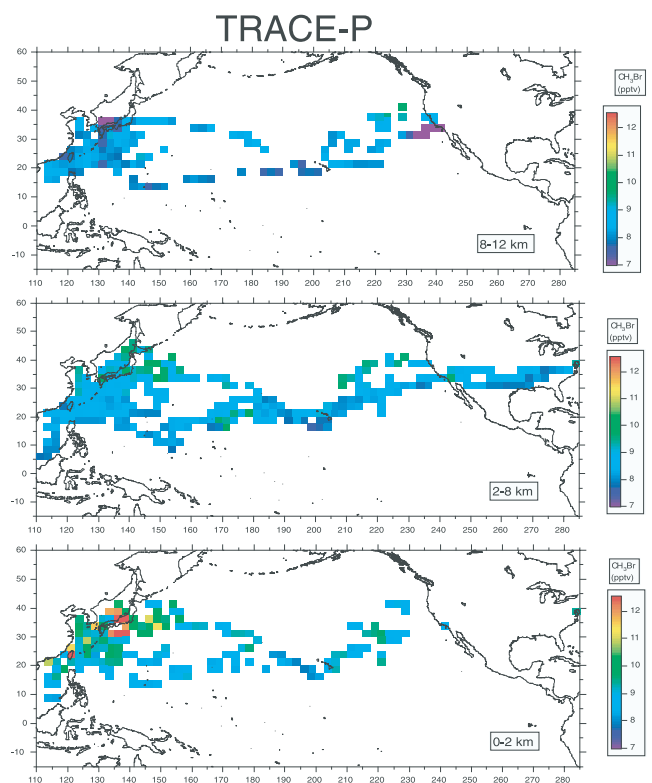

**Figure 6.** Same as Figure 5 but for CH_3Br.
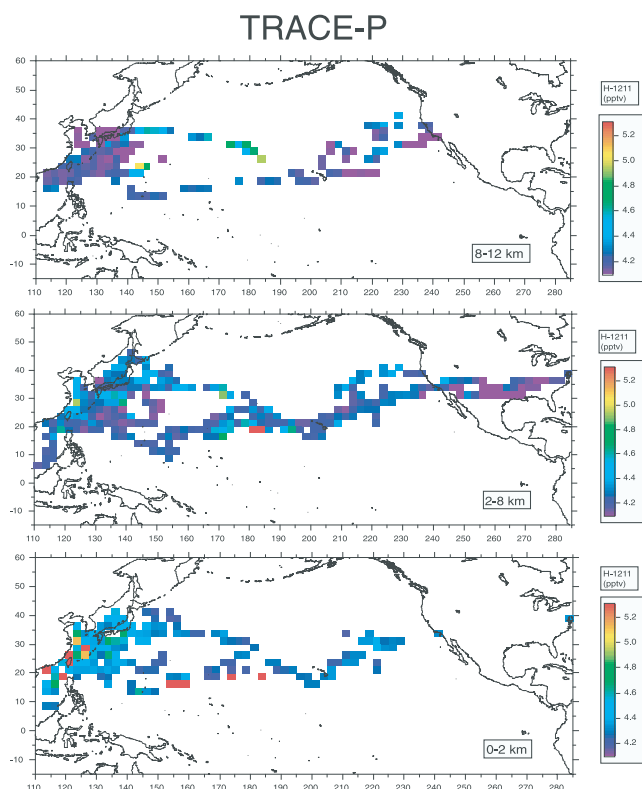
TRACE-P

Figure 7. Same as Figure 5 but for Halon-1211.

evaluating the representativeness of the resulting regional distribution. This is a particularly critical question if the distributions derived during TRACE-P are to be compared to other times or areas (such as PEM-West B). However, when the representativeness of distributions based on the much more sparsely sampled PEM-West A and PEM-West B data sets was examined in detail by *Ehhalt et al.* [1997], they concluded that the distributions were reasonable descriptions of the "true" average pattern of concentrations, despite incomplete and irregular sampling.

[27] A meteorological overview of PEM-West B is given by *Merrill et al.* [1997] and of TRACE-P by *Fuelberg et al.* [2003]. TRACE-P was conducted during the transition months between winter and spring when meteorological conditions were undergoing major seasonal changes, but after comparing both missions, Fuelberg et al. concluded that flow patterns and precipitation during TRACE-P appeared quite similar to those during PEM-West B. However, the different sampling locations, especially over the eastern Pacific, means that the TRACE-P data set could be more influenced by aged Asian outflow that had transited the Pacific and re-circulated in the "river of pollution" [*Blake et al.*, 2001; *Martin et al.*, 2002]. This eastern region may also be influenced by North American outflow to some extent [*Blake et al.*, 2001]. In addition, several TRACE-P flights specifically targeted the Yellow Sea area near China (Figure 1), a region where very strong outflow was encountered (as evidenced by high ethene and ethyne levels) but that was not sampled during PEM-West B (Figures 2 and 3).

[28] Comparison between PEM-West B and TRACE-P is further complicated by the seasonal offset between the two missions. PEM-West B was conducted between 7 February

and 15 March 1994 in the same general geographic area as TRACE-P [*Hoell et al.*, 1997] (Figure 1). However, PEM-West B was slightly shorter and took place approximately 20 days earlier, with an overlap with the TRACE-P period of about 14 days (Figure 10).

[29] For relatively long-lived ethane, its seasonal variation (highest mixing ratios in the winter and lowest in late summer) is a relatively minor consideration, but the rate of springtime decline is more apparent for the shorter-lived hydrocarbons [*Penkett et al.*, 1993; *Blake et al.*, 2003; *Swanson et al.*, 2003]. Seasonal variability is greatest in the high northern latitudes [e.g., *Rudolph*, 1995; *Blake et al.*, 1997, 2003; *Gupta et al.*, 1998], where solar zenith angles, and consequently the photochemistry that drives production of hydroxyl (OH) radicals, are changing rapidly during springtime. Seasonal variability is also more pronounced at lower altitudes [*Blake et al.*, 2003].

[30] *Davis et al.* [2003] employed their time-dependent box model (TDM) to investigate changes in ozone and ozone precursors between PEM-West B and TRACE-P, and calculated average diurnal OH values at sea level to be 4×10^5 cm^{-3} for the PEM-West B period, and as high as 8×10^5 cm^{-3} for TRACE-P. The difference results in a substantial reduction in the estimated lifetimes of the various hydrocarbon species during TRACE-P. However, the effect of higher OH levels will be most evident for species whose lifetimes are shorter than the approximately 3-week seasonal separation time for the two studies. Consistent with this, the low-altitude TRACE-P mixing ratios north of 25°N for ethene (lifetime 2–4 days) are approximately half their PEM-West B values (Figure 9 and Table 1). By comparison, the longer-lived gases such
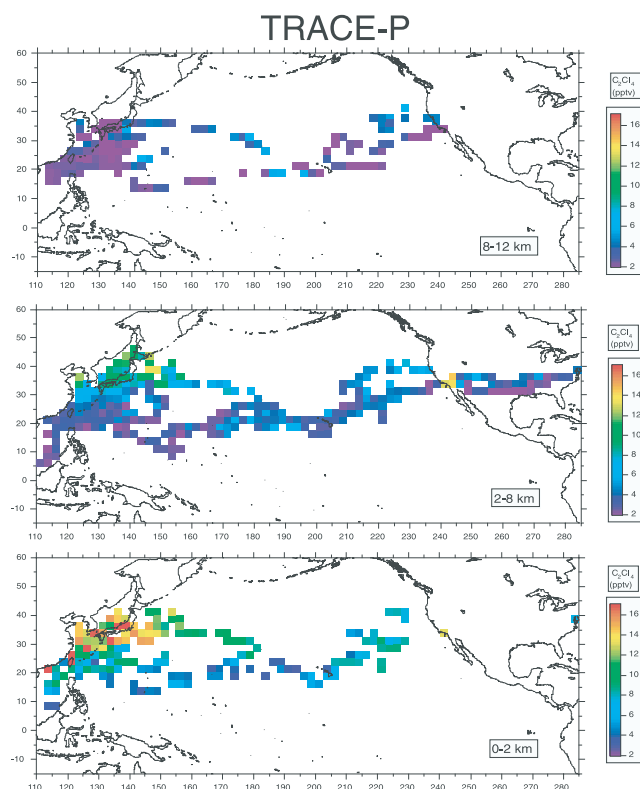
TRACE-P

Figure 8. Same as Figure 5 but for C$_2$Cl$_4$.
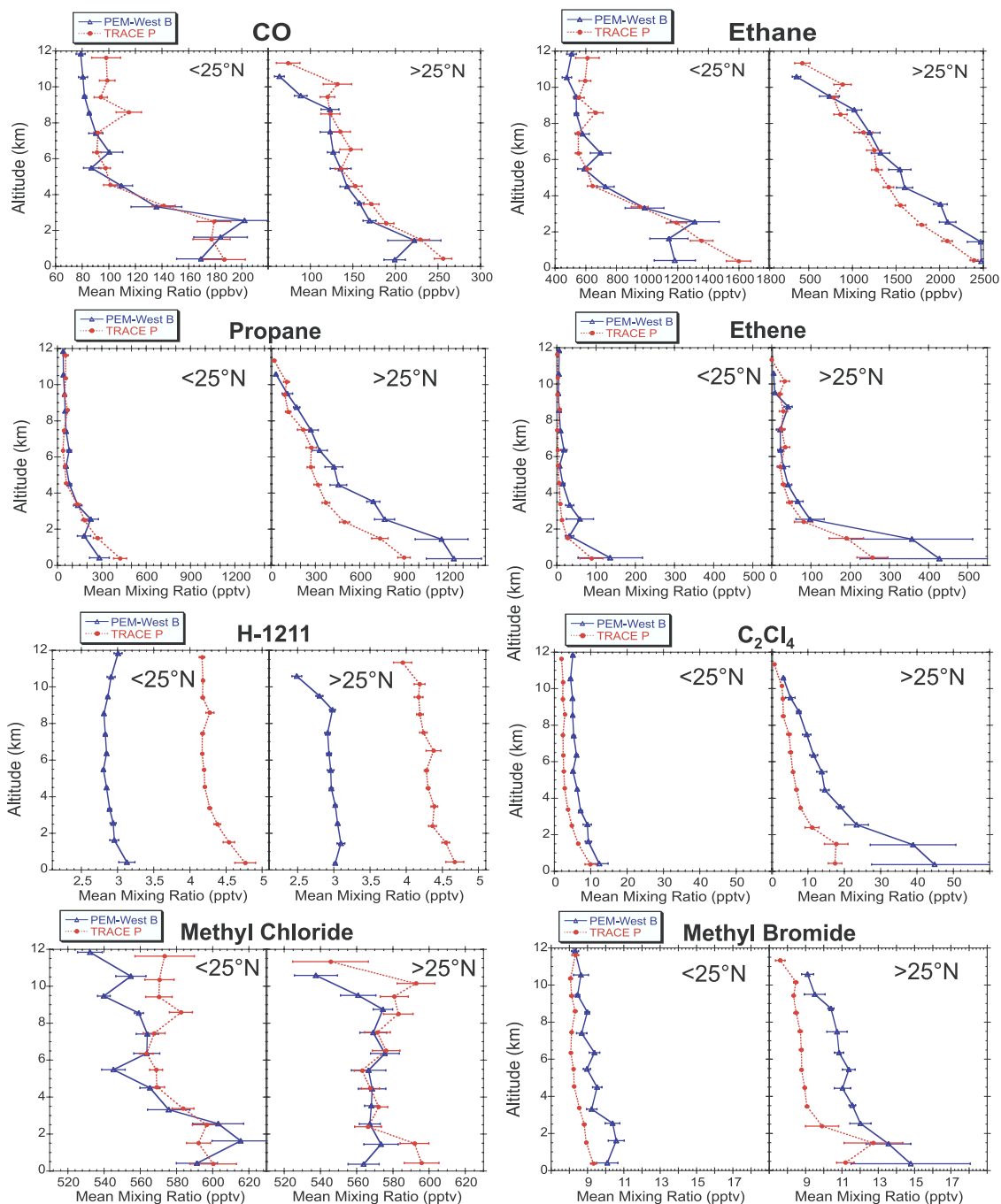
Figure 9. Mean mixing ratios of selected trace gases for 1-km altitude increments for all samples collected west of 165°E for PEM-West B (blue) and TRACE-P (red). Error bars are the 95% confidence level of the mean.

as ethane and CO (which have lifetimes on the order of 2–4 months at this time of year), are not significantly influenced by the 3-week shift (Figures 9 and 11 and Table 1). In support, Table 1 shows that the more northerly PEM-West B air masses were associated with higher ethyne/CO ratios, indicating that they are relatively more fresh (less photochemically aged), likely as the consequence of lower seasonal PEM-West B OH levels. It appears that high-latitude average NMHC mixing ratios were significantly influenced by changing seasonal photochemical conditions.

[31] Most air masses sampled in the middle and upper troposphere during TRACE-P originated from the west, and traveled in the middle latitude band of prevailing westerlies [*Fuelberg et al.*, 2003]. Some backward trajectories passed over highly industrialized regions of Japan and China (e.g., Shanghai and Beijing). A relatively small number of 5-day backward trajectories (as calculated by *Fuelberg et al.* [2003]) passed over southern, central and northern Europe, suggesting that relatively fresh European air masses were sampled infrequently during TRACE-P.

Table 1. Median Mixing Ratios in pptv (Unless Otherwise Stated) for Selected NMHCs, CO and Ozone for 2.5°N Latitude Increments Averaged Over the Western Pacific (West of 165°E) During PEM-West B (PWB) and TRACE-P (TrP)[a]

Latitude Range, °N	Ethane PWB	Ethane TrP	Ethane Delta	Ethene PWB	Ethene TrP	Ethene Delta	Ethyne PWB	Ethyne TrP	Ethyne Delta	Propane PWB	Propane TrP	Propane Delta	Benzene PWB	Benzene TrP	Benzene Delta	CO, ppbv PWB	CO, ppbv TrP	CO, ppbv Delta	ethyne/CO PWB	ethyne/CO TrP	ethyne/CO Delta	Ozone, ppbv PWB	Ozone, ppbv TrP	Ozone, ppbv Delta
0–2 km, <165E																								
7.5–10	862	711	−151	22	29	7	289	190	−100	75	53	−22	51	39	−12	146	110	−36	1.9	1.6	−0.2	26	22	−4
12.5–15	933	812	−121	41	9	−32	319	146	−173	110	79	−31	58	27	−32	145	106	−39	1.8	1.4	−0.4	33	25	−8
15–17.5	1073	1016	−57	8	3	−5	262	221	−41	153	92	−61	45	47	2	133	123	−10	2.0	1.8	−0.2	29	26	−4
17.5–20	2160	968	−1193	118	5	−113	1367	211	−1156	458	113	−345	261	48	−214	336	130	−206	4.1	1.6	−2.5	61	27	−34
20–22.5	2220	1695	−525	319	31	−288	1033	521	−512	809	430	−379	236	114	−122	249	186	−63	4.0	2.6	−1.4	48	46	−1
22.5–25	1983	1515	−468	110	20	−90	746	442	−304	691	321	−371	159	100	−60	203	175	−29	3.7	2.5	−1.1	47	50	3
25–27.5	1965	1747	−217	63	46	−17	620	525	−95	726	540	−187	128	125	−4	162	187	24	3.8	2.9	−0.9	47	51	4
27.5–30	2088	2143	55	80	93	14	713	713	0	773	683	−90	127	173	45	168	208	40	4.2	3.3	−0.9	45	57	12
30–32.5	2338	2352	13	97	85	−12	797	779	−18	928	769	−159	146	211	65	169	234	64	4.4	3.4	−1.1	41	64	23
32.5–35	2601	2003	−598	214	75	−139	1038	618	−420	1113	610	−503	202	174	−28	205	207	1	5.1	3.1	−2.0	43	58	15
35–37.5	2711	2363	−348	341	118	−223	1113	773	−341	1209	819	−390	218	188	−30	204	234	30	5.3	3.5	−1.7	38	58	20
37.5–40	2800	2383	−417	385	65	−320	1142	713	−429	1283	802	−481	228	168	−59	209	189	−20	5.5	3.6	−1.9	39	57	18
40–42.5	2909	2123	−786	340	36	−304	1045	618	−426	1458	704	−754	214	134	−80	207	183	−24	5.0	3.5	−1.6	37	53	16
Average	2049	1679	−370	164	47	−117	806	498	−309	753	463	−290	160	119	−41	195	175	−20	3.9	2.7	−1.2	41	46	4
Std Dev	695	619	353	137	37	126	357	234	311	454	298	220	74	63	72	54	44	66	1.3	0.8	0.7	9	15	15
2–8 km, <165E																								
5–7.5	642	495	−148	6	0	−6	86	72	−14	64	25	−39	15	13	−2	48	31	−18	0.9	1.0	0.1	91	77	−15
7.5–10	680	556	−123	14	1	−13	119	99	−21	63	29	−35	19	16	−3	46	40	−6	1.1	1.1	0.0	104	88	−16
10–12.5	556	564	8	5	0	−5	76	99	23	45	27	−18	8	14	5	51	47	−4	0.9	1.1	0.2	88	88	0
12.5–15	615	604	−11	6	1	−4	90	108	17	53	40	−13	12	19	7	51	46	−5	0.9	1.2	0.2	94	92	−3
15–17.5	634	638	3	5	0	−4	92	106	15	58	43	−15	14	15	1	52	47	−5	1.0	1.2	0.2	94	93	0
17.5–20	593	699	105	5	1	−4	86	158	72	44	73	29	13	26	12	64	50	−15	0.9	1.5	0.5	94	105	10
20–22.5	743	910	167	13	8	−5	155	251	96	86	98	12	30	40	9	50	50	0	1.4	1.8	0.4	106	124	18
22.5–25	1190	832	−358	43	7	−36	426	220	−207	178	107	−71	80	41	−39	47	53	6	2.3	1.8	−0.5	156	120	−36
25–27.5	1459	885	−574	29	12	−17	467	291	−176	391	96	−295	76	51	−25	46	58	11	3.1	1.9	−1.2	153	134	−19
27.5–30	1652	1156	−496	46	13	−33	469	367	−102	447	205	−242	82	63	−18	44	60	16	3.0	2.3	−0.7	144	149	4
30–32.5	1756	1324	−431	39	29	−10	529	369	−159	492	296	−196	88	76	−13	44	61	17	3.5	2.5	−1.0	151	150	−1
32.5–35	1611	1454	−157	30	14	−16	408	357	−50	443	331	−112	67	67	0	46	61	15	3.0	2.5	−0.5	139	146	7
35–37.5	1707	1669	−37	28	49	21	446	429	−17	572	435	−137	64	95	30	44	61	18	3.3	2.7	−0.6	138	161	23
37.5–40	1673	1743	70	33	43	10	430	459	28	541	439	−102	58	101	43	44	60	16	2.9	2.4	−0.5	135	165	30
40–42.5	2063	2116	53	65	45	−20	604	618	14	757	629	−128	96	128	32	43	60	17	3.7	3.2	−0.5	160	180	19
42.5–45	2527	1999	−528	172	39	−133	878	545	−334	1033	624	−410	165	105	−60	41	68	27	4.3	3.2	−1.2	198	172	−26
45–47.5	1926	1725	−201	58	27	−32	566	423	−144	694	463	−231	79	74	−5	56	69	13	3.4	2.7	−0.7	159	153	−5
Average	1296	1139	−156	35	17	−18	349	292	−56	351	233	−118	57	55	−1	48	54	6	2.3	2.0	−0.3	130	129	−1
Std Dev	630	550	238	40	18	33	239	171	114	306	215	122	42	37	25	6	10	13	1.2	0.8	0.5	32	33	18

[a]Delta values are the difference between PWB and TrP values for that latitude band.
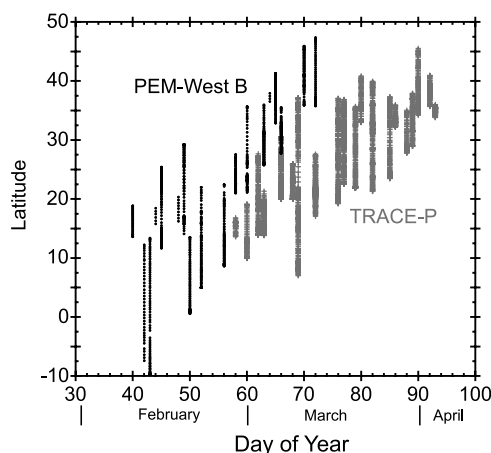
Figure 10. Temporal distribution for whole air samples collected west of 165°E during PEM-West B and TRACE-P.

3.3.2. Long-Term Changes in Halocarbons

[32] As for the NMHCs, the representativeness of the two relatively brief "snapshot" periods of intensive trace gas sampling that comprise TRACE-P and PEM-West B needs to be kept in mind as a background to the following comparisons between halocarbon distributions.

3.3.2.1. Halon-1211

[33] Halon-1211 has been widely used in fire-fighting equipment. The high ozone-depleting potential of this gas (which has an ODP of 3) resulted in its regulation under the Montreal Protocol, with production ceasing in developed countries in 1994 [UNEP, 1991]. Therefore a large fraction of current emissions are thought to arise from the use of the large reserves of material that are stored in existing fire extinguishers [WMO, 2002]. However, the Montreal Protocol allows developing countries until 2010 before they must completely phase out Halon-1211 production and consumption [UNEP, 1991]. China is one of very few countries which still produces Halon-1211, and recent emissions have been associated with the Asian continent [UNEP, 2002; Fraser et al., 1999; Blake et al., 2001]. In fact, the highest TRACE-P mixing ratios (up to 27 pptv) were measured in Chinese outflow downwind of Shanghai (during DC-8 Flight 13, the "Shanghai Plume" event, see Jacob et al. [2003] and Simpson et al. [2003]).

[34] The atmospheric concentration of Halon-1211 has continued to grow over the past few years [Butler et al., 1998; Fraser et al., 1999; Montzka et al., 1999]. Comparison of PEM-West B with the TRACE-P data reveals an average increase of approximately 0.19 ± 0.05 pptv/year over the 7 years between these experiments (Figures 9 and 12 and Table 2). This increase is similar to the 0.16 pptv/yr and 0.21 pptv/yr reported by Butler et al. [1998] and Fraser et al. [1999], respectively, for 1995–1996, and to the 0.20 pptv/yr for early 1998 [Fraser et al., 1999].

3.3.2.2. Methyl Chloroform (CH_3CCl_3)

[35] Our previous analysis of the PEM-West B data [D. R. Blake et al., 1996] employed CH_3CCl_3 as a useful tracer for coastal Asian industrial activity. However, the Montreal Protocol has since required the production of CH_3CCl_3 to be phased out in developed countries, and CH_3CCl_3 emissions are to be frozen in 2003 and phased out by 2015 in developing countries [UNEP, 1991]. The lifetime of CH_3CCl_3 (~4.9 yrs [Prinn et al., 2001]) is relatively short, and the banning legislation has been quickly reflected as a sharp decrease in the atmospheric concentration of CH_3CCl_3 [Prinn et al., 1995; Romashkin et al., 1999] such that TRACE-P mixing ratios are only 1/3 of those measured in 1994 (Table 2). However, the extent to which Asian countries currently produce CH_3CCl_3 is unclear. Even though methyl chloroform was significantly enhanced in certain air masses sampled close to Asia (Figure 13), it was
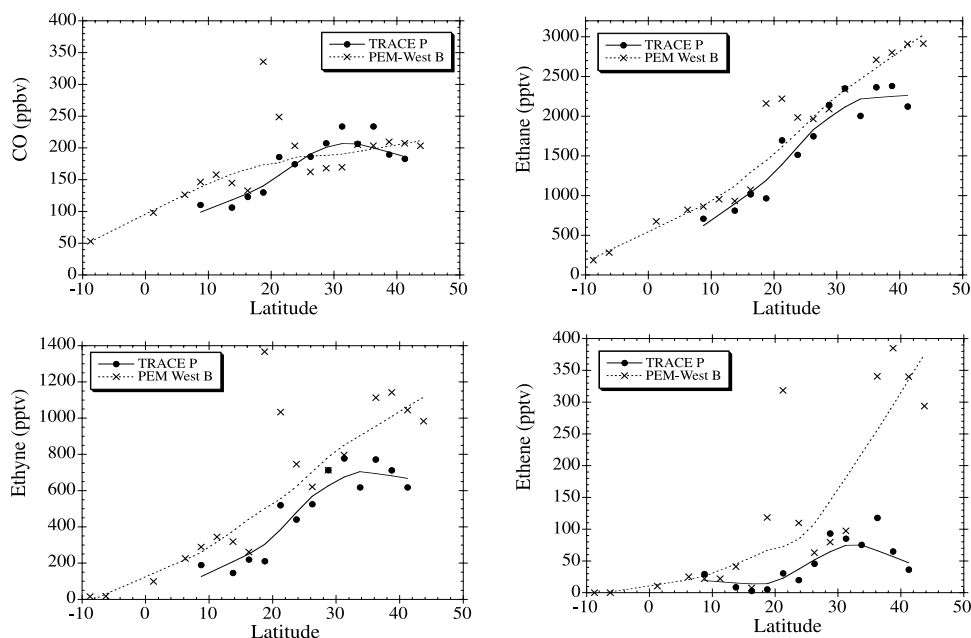

Figure 11. Median CO, ethane, propane and ethene mixing ratio values for the 2.5° × 2.5° latitude/longitude bins for TRACE-P and PEM-West B at low altitudes (<2 km) over the western Pacific (west of 165°E).
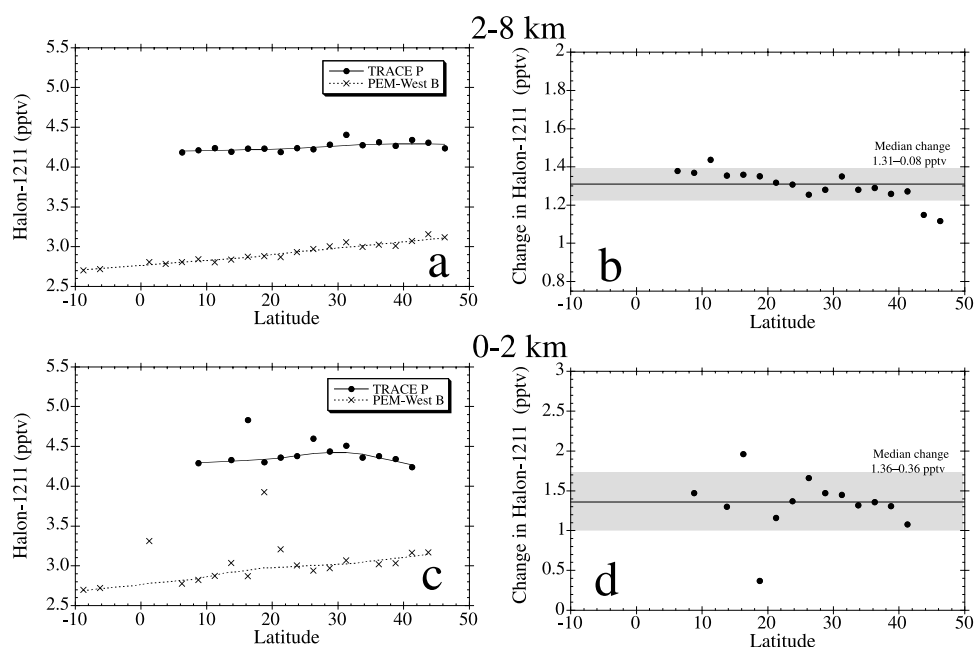
Figure 12. Median mixing ratios of Halon-1211 for 2.5° bins for TRACE- P and PEM-West B over the western Pacific (west of 165°E) for the altitude ranges (a) 2−8 km (c) 0−2 km. Figure 12b and 12d show the difference between the median data in Figures 12a and 12c, respectively, for the two missions (TRACE-P - PEM-West B). The line is the mean difference over all latitudes and the shaded band is the 1 standard deviation uncertainty.

no longer the general indicator of urban air during TRACE-P that it was during PEM-West A [*D. R. Blake et al.*, 1996]. The largest CH_3CCl_3 enhancements were found on landing in Yokota, Japan (up to 87 pptv) and Hong Kong (up to 68 pptv). The next highest mixing ratios (up to 65 pptv) were measured in Chinese outflow during DC-8 Flight 13 (the "Shanghai Plume" event, e.g., *Jacob et al.* [2003] and *Simpson et al.* [2003]). High levels (up to 53 pptv) were also found during a low altitude sampling leg flown close to the west coast of Taiwan during DC-8 Flight 12. Elevated levels of Halon-1211 (to 9 pptv), CFC-11 (to 280 pptv), and CCl_4 (to 126 pptv) were also associated with this Flight 12 plume. In addition, CH_3Cl, OCS and HCN were elevated, indicating mixed influence from biomass burning/biofuel/ coal emissions. The 5-day backward trajectories for the Flight 12 air mass that contained the highest levels of CH_3CCl_3 originated from southwest of the flight track, so during the previous 5 days it had traveled over the coast of southeastern China and Hong Kong. Other trajectories associated with this leg, but with lower CH_3CCl_3 levels, typically originated to the north and northwest of the flight track from the Shanghai region of coastal China.

[36] However, even though some CH_3CCl_3 enhancements were associated with outflow from China, the relatively high ratios of CH_3CCl_3 versus CO for "Japan" (particularly P-3B Flight 14, Plume C whose trajectory passes over Korea and the southern islands of Japan versus "China" (see section 3.4.1)) suggest that China is not the sole remaining source for significant CH_3CCl_3 emissions.

3.3.2.3. Carbon Tetrachloride (CCl_4)

[37] The atmospheric mixing ratio of CCl_4 reached a peak of 104 ± 3 pptv in 1989−1990 [*Simmonds et al.*, 1998], then decreased by 0.7 to 0.9 pptv yr^{-1} between mid-1990 and mid-1998 [*Prinn et al.*, 2000], roughly consistent with

the 7-year decrease of 8.7 pptv reported for low altitudes in Table 2.

[38] Atmospheric CCl_4 levels have declined as a result of the CFC phase-out by non-Article 5(1) Parties. The primary source of atmospheric CCl_4 emissions is from its use as a feedstock to produce CFCs. For 1996 this use was estimated to be about 70 percent of total emissions, with the majority of the emissions from feedstock use thought to originate from CFC production by Article 5(1) Parties [*UNEP*, 1999]. However, phase-out is not mandated by the Montreal Protocol for Article 5(1) countries until 1 January 2005 [*UNEP*, 1991].

[39] Nevertheless, the spatial distribution of CCl_4 (Figure 14) reveals very few "hot spots" where mixing ratios of CCl_4 are elevated over the remarkably constant background levels, even at low altitudes (mean mixing ratio 100.0 ± 0.4 pptv for <2 km, Table 2). In fact, of the 24 TRACE-P samples whose CCl_4 mixing ratios were elevated above 110 pptv, one sample was collected on landing in Yokota, Japan but the remaining samples were collected in Chinese outflow during DC-8 Flights 12 and 13. The highest TRACE-P mixing ratio (162 pptv) was associated with the Shanghai Plume (Flight 13). Unlike CH_3CCl_3, the observation that most CCl_4 enhancements are associated with outflow from China is supported by the relatively high ratios of CCl_4 versus CO for "China" versus "Japan" shown in section 3.5.1.

3.3.2.4. C_2Cl_4

[40] Tetrachloroethene levels have also decreased significantly, especially to the north of 25°N (Figures 9 and 15 and Table 2), likely as the result of increased recycling of C_2Cl_4 [*U.S. Environmental Protection Agency*, 1994] and lower production of CFCs, some of which are derived from C_2Cl_4. However continued use of C_2Cl_4 in Asia, in addition to its

Table 2. Median Mixing Ratios in pptv (Unless Otherwise Stated) for Selected Halocarbons for 2.5°N Latitude Increments Averaged Over the Western Pacific (West of 165°E) During PEM-West B (PWB) and TRACE-P (TrP)[a]

Latitude Range, °N	CFC-12			CFC-11			H-1211			CH₃CCl₃			CCl₄			C₂Cl₄			CH₃Cl			CH₃Br		
	PWB	TrP	Delta	PWB	TrP	Delta	PWB	TrP	Delta	PWB	TrP	Delta	PWB	TrP	Delta	PWB	TrP	Delta	PWB	TrP	Delta	PWB	TrP	Delta
										0–2 km, <165E														
7.5–10	518	538	**21**	273	261	**−13**	2.8	4.3	**1.5**	127	39	**−87**	108.4	99.4	**−9.0**	7.6	3.7	**−3.8**	618	580	**−38**	10.1	8.3	**−1.9**
12.5–15	522	540	**18**	278	261	**−17**	3.0	4.3	**1.3**	126	40	**−86**	108.1	99.2	**−8.9**	8.7	4.4	**−4.3**	600	564	**−36**	9.9	8.5	**−1.4**
15–17.5	514	539	**25**	275	261	**−14**	2.9	4.8	**2.0**	131	40	**−91**	108.6	99.7	**−8.9**	10.8	5.9	**−4.9**	573	563	**−10**	9.7	8.8	**−0.9**
17.5–20	520	539	**19**	276	261	**−15**	3.9	4.3	**0.4**	126	40	**−86**	108.0	99.2	**−8.8**	13.3	4.8	**−8.6**	662	549	**−113**	12.3	8.6	**−3.7**
20–22.5	524	539	**15**	278	262	**−16**	3.2	4.4	**1.2**	134	41	**−94**	110.1	100.1	**−10.1**	20.9	8.3	**−12.6**	624	569	**−55**	12.8	9.1	**−3.7**
22.5–25	523	539	**16**	277	261	**−16**	3.0	4.4	**1.4**	132	41	**−91**	108.5	100.3	**−8.3**	17.6	7.6	**−10.0**	579	571	**−8**	11.0	9.1	**−2.0**
25–27.5	522	540	**17**	276	262	**−14**	2.9	4.6	**1.7**	137	41	**−96**	108.7	100.2	**−8.4**	22.9	9.1	**−13.8**	552	577	**25**	10.4	9.4	**−1.0**
27.5–30	522	539	**17**	275	262	**−13**	3.0	4.4	**1.5**	138	41	**−97**	108.3	100.3	**−8.0**	23.4	11.3	**−12.1**	561	571	**10**	11.9	9.1	**−2.7**
30–32.5	521	541	**20**	275	263	**−12**	3.1	4.5	**1.4**	131	42	**−89**	108.2	101.1	**−7.2**	22.3	15.1	**−7.1**	554	597	**43**	11.9	9.7	**−2.2**
32.5–35	524	540	**16**	276	262	**−14**	3.0	4.4	**1.3**	137	41	**−96**	109.0	100.2	**−8.8**	29.2	13.4	**−15.8**	550	554	**4**	12.2	9.8	**−2.4**
35–37.5	524	540	**17**	276	263	**−13**	3.0	4.4	**1.4**	133	42	**−91**	109.4	100.3	**−9.1**	24.0	13.2	**−10.8**	567	566	**−1**	11.7	9.8	**−1.9**
37.5–40	523	538	**15**	276	261	**−14**	3.0	4.3	**1.3**	131	42	**−90**	108.6	99.6	**−8.9**	22.5	12.4	**−10.1**	551	546	**−4**	11.5	10.0	**−1.5**
40–42.5	526	541	**15**	277	262	**−15**	3.2	4.2	**1.1**	131	42	**−89**	109.4	100.1	**−9.2**	22.4	11.6	**−10.8**	556	538	**−18**	11.9	9.3	**−2.7**
Average	522	540	**18**	276	262	**−14**	3.1	4.4	**1.3**	132	41	**−91**	108.7	100.0	**−8.7**	18.9	9.3	**−9.6**	580	565	**−15**	11.3	9.2	**−2.1**
Std Dev	3	1	**3**	1	1	**1**	0.3	0.2	**0.4**	4	1	**4**	0.6	0.5	**0.7**	6.7	3.8	**3.7**	35	16	**39**	1.0	0.5	**0.9**
										2–8 km, <165E														
5–7.5	518	539	**21**	276	260	**−15**	2.8	4.2	**1.4**	126	39	**−87**	107.8	98.3	**−9.5**	6.1	2.4	**−3.7**	570	562	**−8**	8.8	7.8	**−1.0**
7.5–10	518	539	**21**	277	260	**−16**	2.8	4.2	**1.4**	124	39	**−85**	107.3	98.8	**−8.5**	6.5	2.5	**−4.0**	575	557	**−18**	9.5	8.0	**−1.5**
10–12.5	519	541	**22**	274	262	**−12**	2.8	4.2	**1.4**	123	40	**−83**	106.9	99.3	**−7.7**	5.1	2.6	**−2.5**	551	566	**15**	9.3	8.3	**−1.0**
12.5–15	517	539	**22**	274	261	**−13**	2.8	4.2	**1.4**	123	39	**−84**	107.2	99.0	**−8.2**	5.3	2.9	**−2.4**	554	561	**7**	8.7	8.2	**−0.5**
15–17.5	515	537	**21**	274	261	**−14**	2.9	4.2	**1.4**	126	39	**−86**	107.5	99.0	**−8.5**	5.8	3.4	**−2.5**	565	556	**−9**	9.0	8.3	**−0.7**
17.5–20	517	537	**20**	274	260	**−14**	2.9	4.2	**1.4**	124	39	**−85**	107.5	98.7	**−8.8**	5.4	3.1	**−2.4**	559	565	**6**	9.2	8.2	**−0.9**
20–22.5	519	537	**18**	274	260	**−14**	2.9	4.2	**1.3**	120	39	**−81**	106.9	99.1	**−7.8**	6.2	3.5	**−2.7**	574	580	**6**	9.5	8.5	**1.0**
22.5–25	519	536	**16**	275	259	**−15**	2.9	4.2	**1.3**	122	39	**−83**	107.5	98.8	**−8.7**	8.0	3.5	**−4.6**	587	573	**−14**	10.5	8.5	**−2.0**
25–27.5	521	535	**14**	275	259	**−16**	3.0	4.2	**1.3**	128	39	**−89**	108.0	98.4	**−9.6**	13.7	3.3	**−10.4**	572	577	**5**	10.7	8.6	**−2.1**
27.5–30	523	536	**13**	275	260	**−16**	3.0	4.3	**1.3**	128	40	**−88**	108.5	99.1	**−9.4**	14.5	4.8	**−9.7**	573	577	**4**	11.6	8.8	**−2.8**
30–32.5	522	535	**13**	274	259	**−15**	3.1	4.4	**1.4**	126	40	**−86**	106.8	98.8	**−8.0**	16.3	6.4	**−9.9**	587	570	**−17**	12.2	8.9	**−3.3**
32.5–35	521	537	**16**	273	260	**−13**	3.0	4.3	**1.3**	125	40	**−85**	107.0	98.7	**−8.3**	15.2	7.2	**−8.0**	607	552	**−55**	12.1	8.9	**−3.2**
35–37.5	523	538	**15**	274	260	**−14**	3.0	4.3	**1.3**	127	41	**−87**	106.8	99.6	**−7.2**	17.4	9.4	**−7.9**	564	564	**−1**	11.9	9.4	**−2.5**
37.5–40	523	537	**14**	274	260	**−14**	3.0	4.3	**1.3**	125	40	**−85**	108.9	98.9	**−8.0**	15.3	8.4	**−6.9**	554	548	**−6**	11.4	8.8	**−2.5**
40–42.5	524	539	**14**	274	261	**−13**	3.1	4.3	**1.3**	129	41	**−87**	99.6	99.6	**−7.6**	20.3	10.4	**−9.9**	558	548	**−10**	11.8	9.3	**−2.5**
42.5–45	526	535	**9**	274	259	**−16**	3.2	4.3	**1.2**	128	41	**−87**	98.9	98.9	**−8.5**	21.2	11.2	**−9.9**	564	544	**−21**	11.8	9.5	**−2.3**
45–47.5	524	532	**8**	274	257	**−17**	3.1	4.2	**1.1**	127	40	**−86**	97.9	97.9	**−9.2**	16.2	10.2	**−6.1**	565	541	**−24**	11.6	9.5	**−2.1**
Average	521	537	**16**	274	260	**−15**	3.0	4.3	**1.3**	125	40	**−86**	107.3	98.9	**−8.5**	11.7	5.6	**−6.1**	569	561	**−8**	10.6	8.7	**−1.9**
Std Dev	3	2	**4**	1	1	**1**	0.1	0.1	**0.1**	2	1	**2**	0.5	0.4	**0.7**	5.8	3.2	**3.2**	14	12	**17**	1.3	0.5	**0.9**

[a] Delta values are the difference between PWB and TrP values for that latitude band.
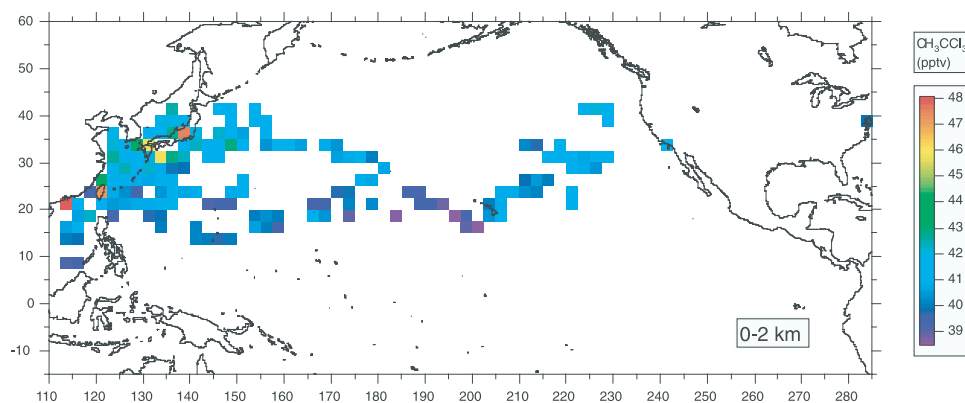
Figure 13. Low-altitude (0–2 km) regional distributions of CH$_3$CCl$_3$ during TRACE-P illustrated as 2.5° × 2.5° latitude/longitude patches color-coded by average mixing ratio.

relatively short lifetime compared to CH$_3$CCl$_3$ (giving rise to low background C$_2$Cl$_4$ mixing ratios), means that it remains a useful indicator of northern industrial emissions.

3.3.2.5. Methyl Chloride (CH$_3$Cl)

[41] Methyl chloride, which is long-lived in the atmosphere (lifetime ~1.3 years), showed no evidence for a significant long-term change between PEM-West B and TRACE-P (Figures 9 and 16, and Table 2). The major sources of methyl chloride are biomass burning and especially biofuel use, which is ubiquitous in Southeast Asia and much of China. An additional contribution from coal burning may also be significant, but more work needs to be done to characterize the potential contribution from this source.

[42] Methyl chloride levels to the south of 25°N and the altitude range 1–2 km were higher during PEM-West B than TRACE-P (Figure 9). Much of this difference can be attributed to the large biomass burning plume (shown in Figure 4) that was encountered during PEM-West B [*D. R. Blake et al.*, 1996; *Talbot et al.*, 1997]. By contrast, transport from the principal biomass burning regions was largely restricted to middle to high altitudes during TRACE-P [*Liu et al.*, 2003].

[43] The generally higher TRACE-P boundary layer (BL) CH$_3$Cl values north of 25°N (Figure 9) are likely a function of the different areas targeted by sampling. TRACE-P included mixed outflow samples that were much closer to the coast of China. By contrast, during PEM-West B the high-latitude (>25°N) BL outflow was mainly of northerly anthropogenic origin [*D. R. Blake et al.*, 1996; *Bey et al.*, 2001] and therefore would be expected to contain lower CH$_3$Cl mixing ratios.

[44] *Heald et al.* [2003] suggest that biomass burning in Southeast Asia over the TRACE-P period was near its seasonal peak. *Liu et al.* [2003] employed a global three-dimensional chemical tracer model (GEOS-CHEM CTM) driven by assimilated meteorological observations to show that outflow from this Southeast Asian biomass burning took place mostly by deep convection. However, northward transport, frontal lifting, and mixing with the anthropogenic outflow also played a role. They concluded that BL outflow over the western Pacific was largely devoid of biomass burning influence. Therefore enhanced TRACE-P CH$_3$Cl averages at high-altitude relative to PEM-West B may be the result of emissions from a more active biomass burning season being uplifted then undergoing fast long-range transport into the Pacific region.

3.3.2.6. Methyl Bromide (CH$_3$Br)

[45] A systematic decrease in CH$_3$Br during the past decade has recently been reported [*Yokouchi et al.*, 2002, *Montzka et al.*, 2002]. We also observed significantly lower mixing ratios of CH$_3$Br between 0 and 2 km (a difference of 2.1 ± 0.9 pptv) between PEM-West B and TRACE-P (Figures 9 and 17, Table 2). Average decreases were 18.5 ± 6.4% for all latitude bins in the 0–2 km layer and 17.1 ± 6.6% for 2–8 km. This is consistent with changes in the global
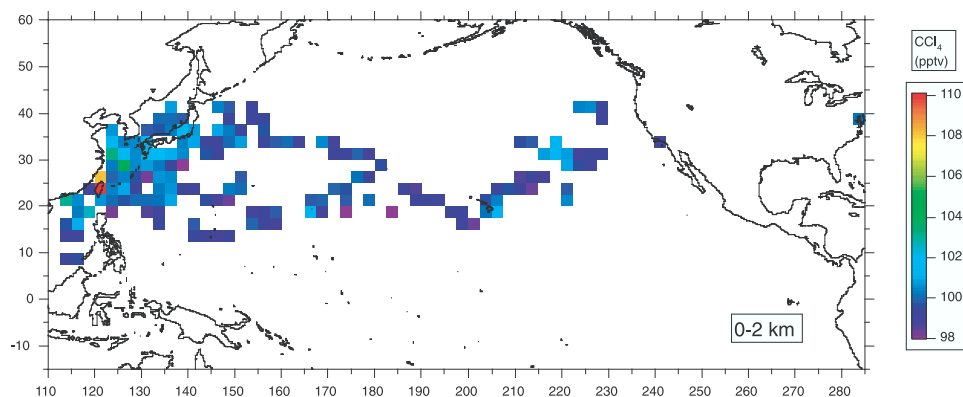

Figure 14. Same as Figure 13 but for CCl$_4$.
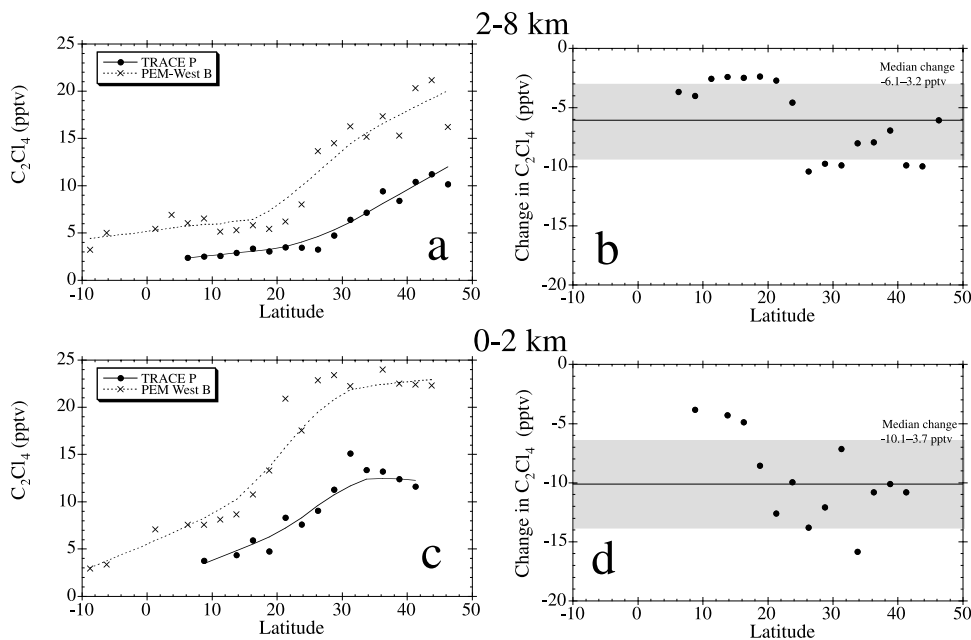
Figure 15. Same as Figure 12 but for C_2Cl_4.

industrial production of methyl bromide reported to UNEP, which was down by 25% in 1999 (compared with 1991 levels) [*UNEP*, 1999]. They are also in line with the results of *Yokouchi et al.* [2002], who estimated that production restrictions outlined in the Montreal Protocol, combined with the relatively short lifetime of CH_3Br (0.32–1.3 yr [*WMO*, 1999]), could be responsible for an approximately 6–22% decrease in NH CH_3Br mixing ratios between 1991 and spring 2001.

[46] The largest reductions observed between PEM-West B and TRACE-P were in general at middle to high latitudes in the 2–8 km altitude range. The average decrease for the 22.5–47.5°N latitude band was 22 ± 3% (Table 2). The change was less systematic for the 0–2 km altitude range, mostly the result of the relatively high variability in methyl bromide mixing ratios during PEM-West B (Table 2). This high PEM-West B variability may be a function of the previously larger emissions [e.g., *Colman et al.*, 2001; *Johnston et al.*, 2002]. The midlatitude location of the largest change in the 2–8 km altitude bin is consistent with the biggest use decrease having taken place in the highly populated midlatitude industrial regions. The observation that this reduction was greater at higher altitudes may also indicate that the principal use changes took place in regions
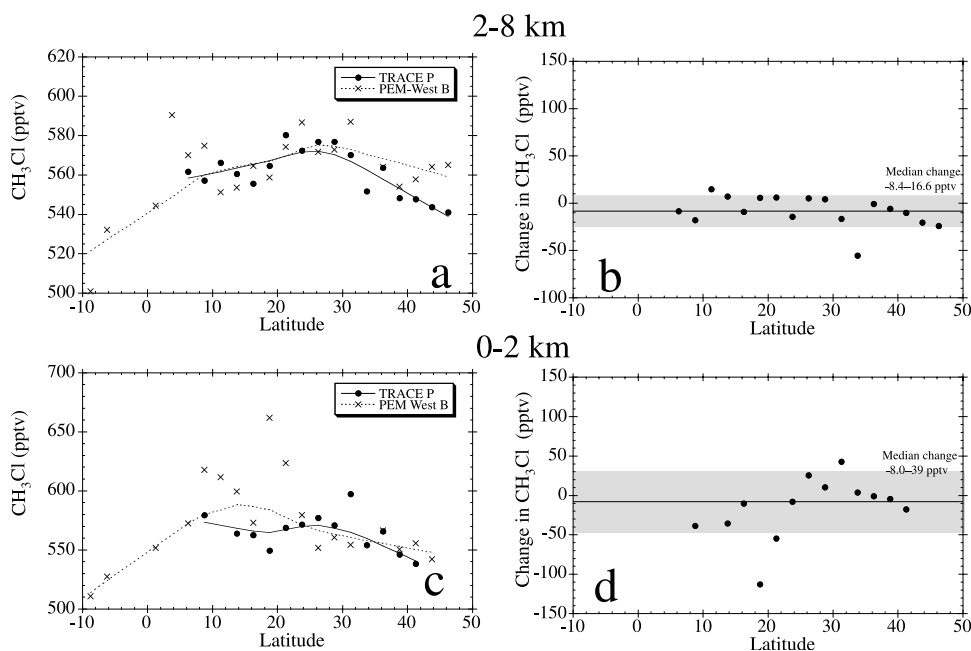
Figure 16. Same as Figure 12 but for CH_3Cl.
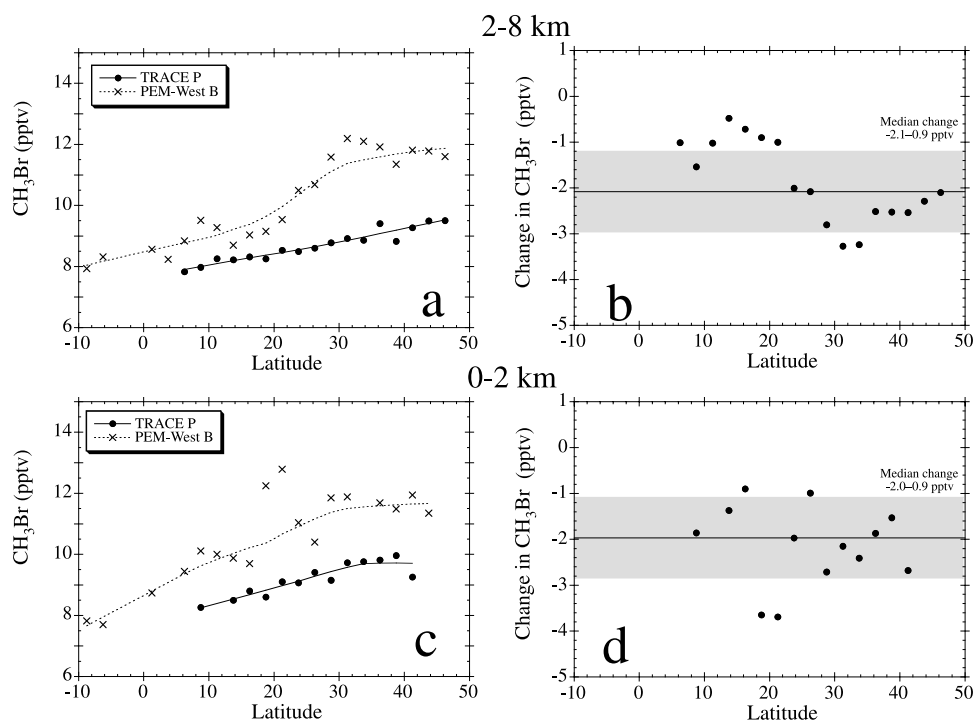
Figure 17. Same as Figure 12 but for CH_3Br.

somewhat removed from the Pacific Rim. For example crop fumigation was previously widespread, but is now regulated in the continental U.S. in accord with the Montreal Protocol and its Amendments.

3.4. Tracers of Asian Outflow: Air Mass Characterization

[47] The following case studies of individual Asian plumes and air mass classification, combined with backward trajectory analysis, help to characterize the origins of some of the wide variety of trace gas-enhanced air masses encountered during TRACE-P.

3.4.1. Methyl Bromide Emissions During TRACE-P

[48] In order to investigate emissions of methyl bromide during TRACE-P more closely, we employed two different air mass classification techniques. Many different air mass characterization methods have been employed to assess the composition of Asian outflow, such as those used on the PEM-West A and B data [e.g., *Smyth et al.*, 1996; *Hoell et al.*, 1997]. *Jordan et al.* [2003], *Russo et al.* [2003], and *Talbot et al.* [2003] all use the same classification scheme based on the backward trajectories of the air masses sampled from the DC-8 during TRACE-P. However, the resolution of this scheme (based on the aerosol data merge) was not high enough to resolve the relatively small-scale variation in CH_3Br by region described above. Instead, we chose to examine a region of particularly high mean CH_3Br mixing ratios near Japan and compare it with a region of similar latitude closer to China (Figure 18). Methyl bromide (and many other gases) was often highly elevated on landing at Yokota, Japan. As this may have been the result of very localized sources, these landing samples were removed from the following analysis.

[49] The correlation plots of selected gases versus CO for the two different regions show CH_3Br, C_2Cl_4, CH_3CCl_3,

and the CFC replacement HCFC-141b to be strongly enhanced relative to CO in many of the samples that were collected close to Japan, compared with those collected in outflow from China (Figure 19). Typical backward trajectories for the enhanced Japan samples (see case studies below) passed over South Korea (and specifically the Seoul region) at low altitude less than 1 day prior to being sampled. The rapidly developing Seoul-Inchon-Suwon triangle delta area is the largest industrial zone in South Korea. Inchon port, just west of Seoul provides one of the few ports along the Yellow Sea to the west and is the largest trade hub in South Korea. Approximately 12% of the global consumption of CH_3Br is used for treating durable commodities and about 3% for treating structures. In 1996 quarantine and preshipment use was equivalent to 22% of global CH_3Br use [*UNEP*, 1998b]. Quarantine and preshipment fumigation is exempt from control under the Montreal Protocol. Moreover, this use appears to be increasing for both developing and developed countries [*UNEP*, 1998b].

[50] By contrast, Halon-1211 and CH_3Cl were most enhanced relative to CO in the Chinese coastal air masses (Figure 19) consistent with previously described signatures of outflow from China. Propane is poorly correlated with CO in both regions, whereas benzene (a general tracer of combustion, similar to CO and ethyne) is well correlated with CO (Figure 19).

3.4.2. Quantitative Analysis of Emissions

[51] For a more quantitative analysis of emissions we adopted an air mass classification scheme based on the one devised by *Kita et al.* [2002]. This scheme allowed us to link the air mass signatures with the different regions/countries and compare them to the emissions inventory data published by *Streets et al.* [2003].

[52] The paths of kinematic trajectories backwards from the sampling points of the two NASA aircraft were exam-
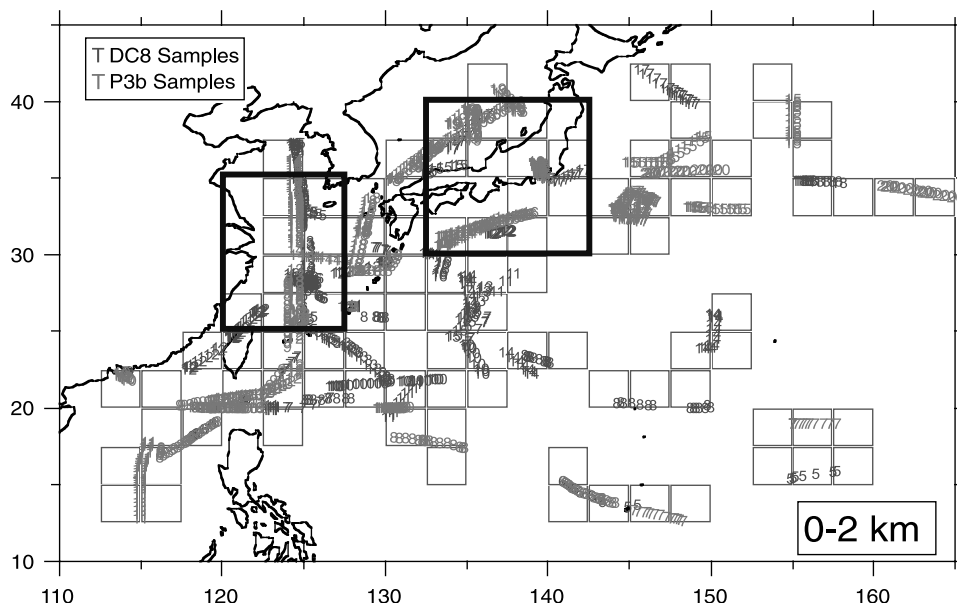
Figure 18. Location of all whole air samples collected between 0 and 2 km and west of 165°E on the NASA P-3B (light grey) and the NASA DC-8 (dark grey) during TRACE-P. The numbers represent flight number. The black boxes represent the "Japan Coast" (RHS) and "China Coast" (LHS) sample subsets.

ined. If a trajectory stayed below 800 hPa pressure level (for SE Asia case: below 450 hPa) for more than 6 hours in one of the four source regions (North China, South China, Japan + Korea, and SE Asia) shown in Figure 20, the air mass was retained in our analysis and classified accordingly. If the trajectory stayed in two regions more than 6 hours, the air mass was excluded.

3.4.2.1. NMHCs

[53] Plots of the light NMHCs versus CO for the four air mass classifications show a similar relationship for ethyne
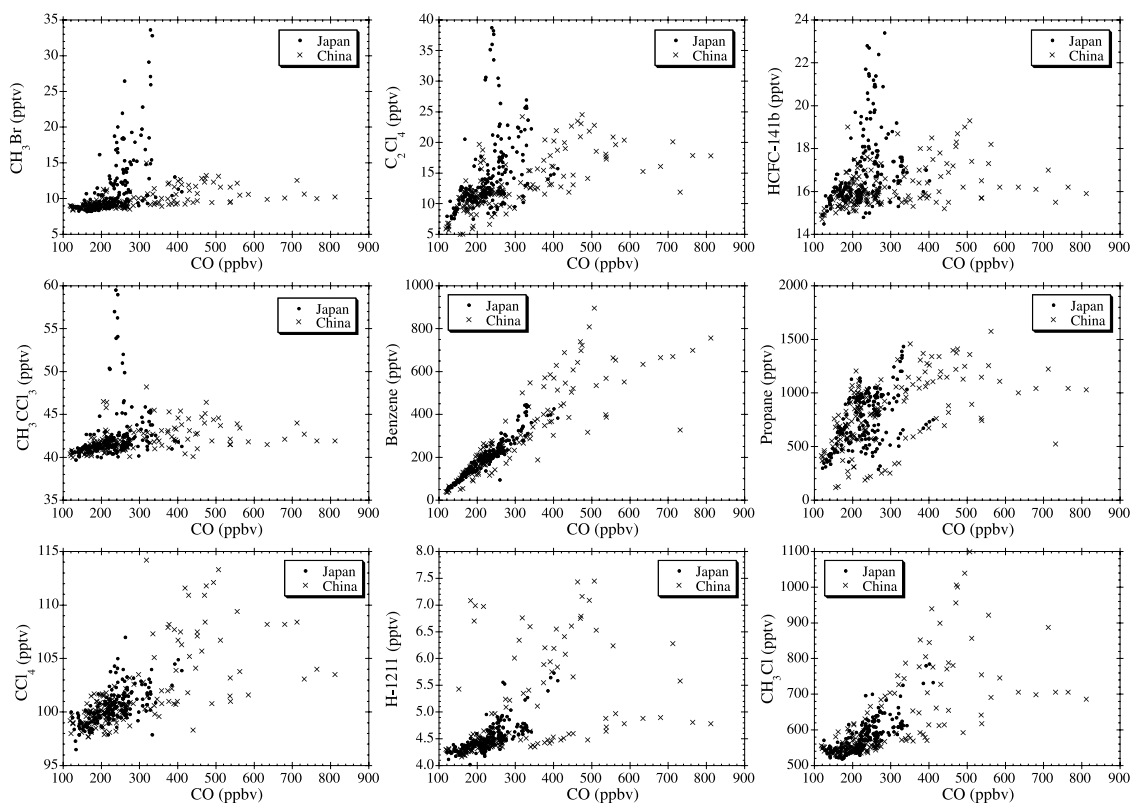
Figure 19. Correlation versus CO for samples collected near the coast of Japan (30–40°N, 135–142.5°E with landing samples removed) and off the coast of China (25–35°N, 120–127.5°E) as shown in Figure 18.
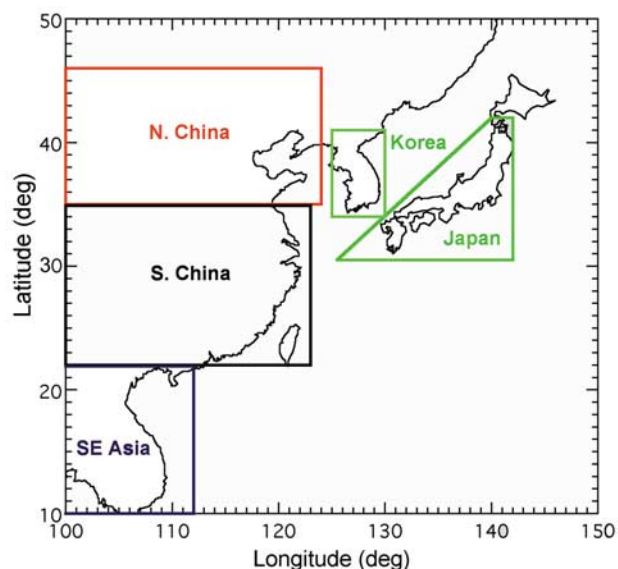
Figure 20. TRACE-P Source Region Classifications from *Kita et al.* [2002]. Note: Japan and Korean classifications are combined in this analysis.

versus CO and very tight correlations (R ≥ 0.92), regardless of air mass type (Figure 21). This is in accord with previous observations that CO and ethyne emissions are very closely linked, for all types and stages of combustion [e.g., *Blake et*

al., 1996]. The relationships of ethane and propane with CO were most similar for the SE Asian and S China classifications (Figure 21). The slopes for both gases were significantly higher for the Japan + Korea classification, with the N. China air masses appearing to be mixed (Figure 21).

[54] "Best guess" emissions for these gases were calculated employing the NMHC/CO ratios in Figure 21 scaled to the CO emission inventory for 2000 from *Streets et al.* [2003] (CO for N and S China was increased by 30% in accord with the findings of *Palmer et al.* [2003a]). Inventory emissions for the NMHCs are taken directly from *Streets et al.* [2003] and compared with the CO-based estimates in Table 3.

[55] Agreement between emission inventory and CO-based estimates is quite good for the Japan + Korea category, especially considering the difficulties and large uncertainties associated with assembling emission inventories for CO and for the NHMCs (as discussed by *Streets et al.* [2003], *Palmer et al.* [2003a] and *Carmichael et al.* [2003]). The South China estimates are also quite close (within about 50%), but the CO-based estimates are always lower. The CO-based estimates for North China are also low, but the propane values are only within a factor of 3, likely because of the highly variable air masses that were sampled for this classification (Figure 21).

[56] There does appear to be a systematic bias towards low CO-based estimates (by a factor of 2–3) for the SE Asian classification, even though correlations of the NMHCs with CO are quite good (R ≥ 0.8). *Heald et al.* [2002] report that
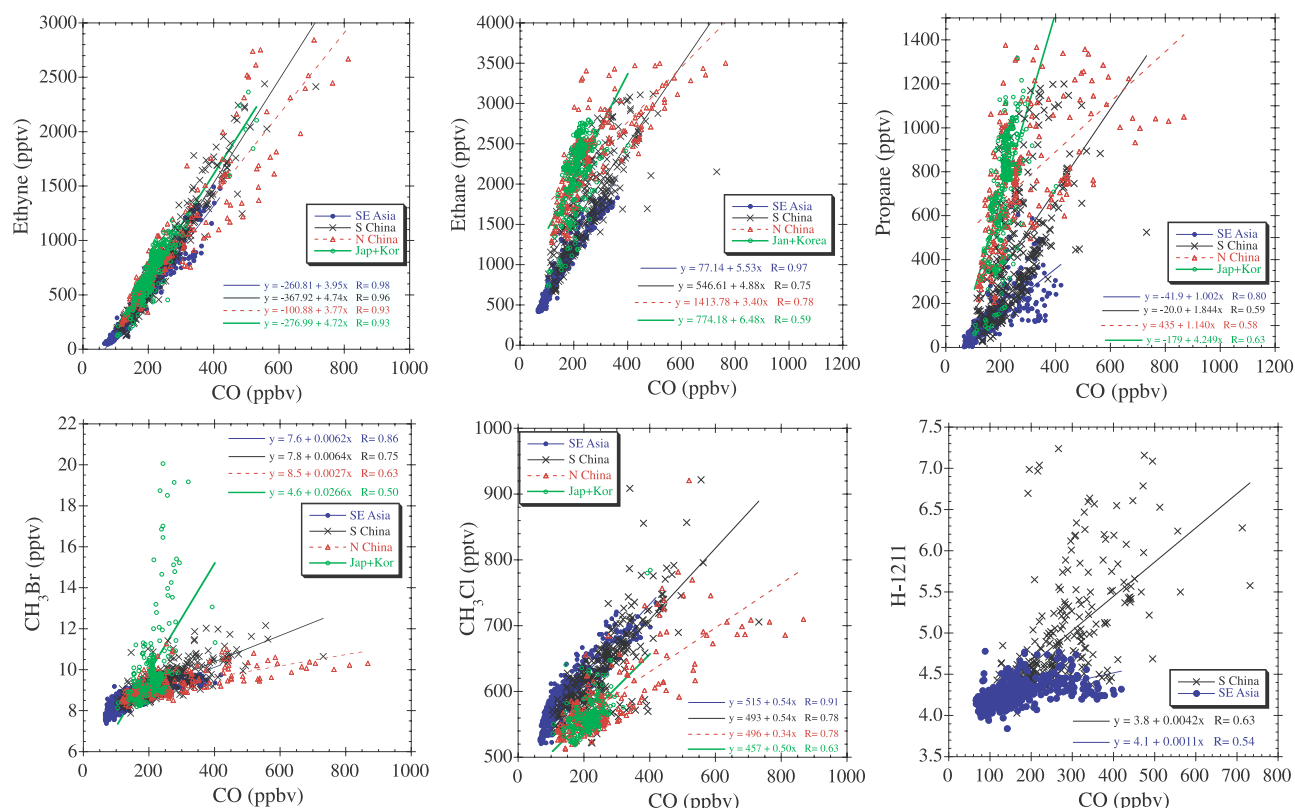

Figure 21. Selected trace gas mixing ratios versus CO for classifications SE Asia, South China, North China, and Japan + Korea as shown in Figure 20 (and see text). Note: The top 5% of data have been removed to better represent regional averages.

Table 3. Selected Trace Gas Mixing Ratios Versus CO for Classifications SE Asia, South China, North China, and Japan and Korea as Shown in Figure 20 (and See Text)[a]

	Ethane			Ethyne			Propane			Methyl Bromide		Methyl Chloride		Halon-1211	
	Ratio versus CO (v/v) ×10^{-6}	Calc. Emission (Gg)	Inventory Emission (Gg)	Ratio versus CO (v/v) ×10^{-6}	Calc. Emission (Gg)	Inventory Emission (Gg)	Ratio versus CO (v/v) ×10^{-6}	Calc. Emission (Gg)	Inventory Emission (Gg)	Ratio versus CO (v/v) ×10^{-6}	Calc. Emission (Gg)	Ratio versus CO (v/v) ×10^{-6}	Calc. Emission (Gg)	Ratio versus CO (v/v) ×10^{-6}	Calc. Emission (Gg)
SE Asia	5.5	144	290	4.0	89	205	1.0	38	103	6.2	0.5	0.54	24	0.0011	0.2
S China	4.9	483	613	4.7	406	567	1.8	267	404	6.4	2.0	0.54	90	0.0042	2.3
N China	3.4	222	363	3.8	213	331	1.1	109	288	2.7	0.6	0.34	37	NC	NC
Japan and Korea	6.5	124	64	4.7	78	52	4.2	119	79	26.6	1.6	0.50	16	NC	NC

[a]"Calc. Emission" is emission based on the measured trace gas/CO ratios from Figure 21, with CO scaled to the *Streets et al.* [2003] CO inventory for 2000 (CO for North and South China was increased by 30% in accord with the findings of *Palmer et al.* [2003a]). Inventory emissions are taken from *Streets et al.* [2003]. NC = not correlated.
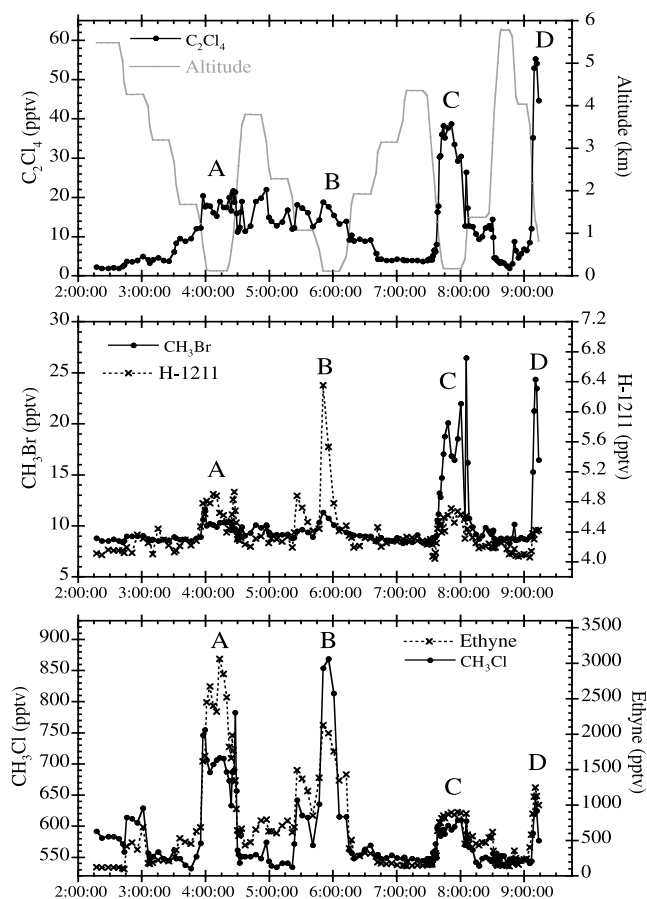

Figure 22. Mixing ratios of selected trace gases versus time for TRACE-P P-3B Flight 14 transit from Okinawa to Yokota, (near Tokyo). The different low altitude plumes are marked A–D.

CO emissions from this region appear to have been underestimated, maybe by as much as 300%. However, emissions of both CO and the NMHCs in this region were dominated by biomass burning during TRACE-P, so it is difficult to understand how such an underestimate could have applied only to CO and not the NMHCs.

3.4.2.2. Methyl Bromide and Methyl Chloride

[57] The plot of CH_3Br versus CO for the four air mass classifications (Figure 21) shows elevated levels of CH_3Br associated with the Japan + Korea classification in accord with the findings discussed earlier (and illustrated in Figure 18). As a consequence of this high ratio, estimated emissions of CH_3Br from Japan + Korea are almost as large as for all of South China (Table 3).

[58] The slopes of CH_3Br versus CO and CH_3Cl versus CO for SE Asia and South China are virtually identical (Figure 21 and Table 3). They are also within the ranges measured in Brazilian and African biomass burning plumes [*Blake et al.*, 1996; *Andreae et al.*, 1996]. Values of 0.28×10^{-6} (R = 0.78) and 0.31×10^{-6} (R = 0.73) for CH_3Br versus CO_2 for SE Asia and South China, respectively (not shown), are also consistent with a biomass burning source of CH_3Br dominating regional emissions of this gas [*Blake et al.*, 1996; *Andreae et al.*, 1996]. The North China data reveal lower slopes versus CO for both CH_3Br and CH_3Cl compared with South China and SE Asia. The lower slope indicates that
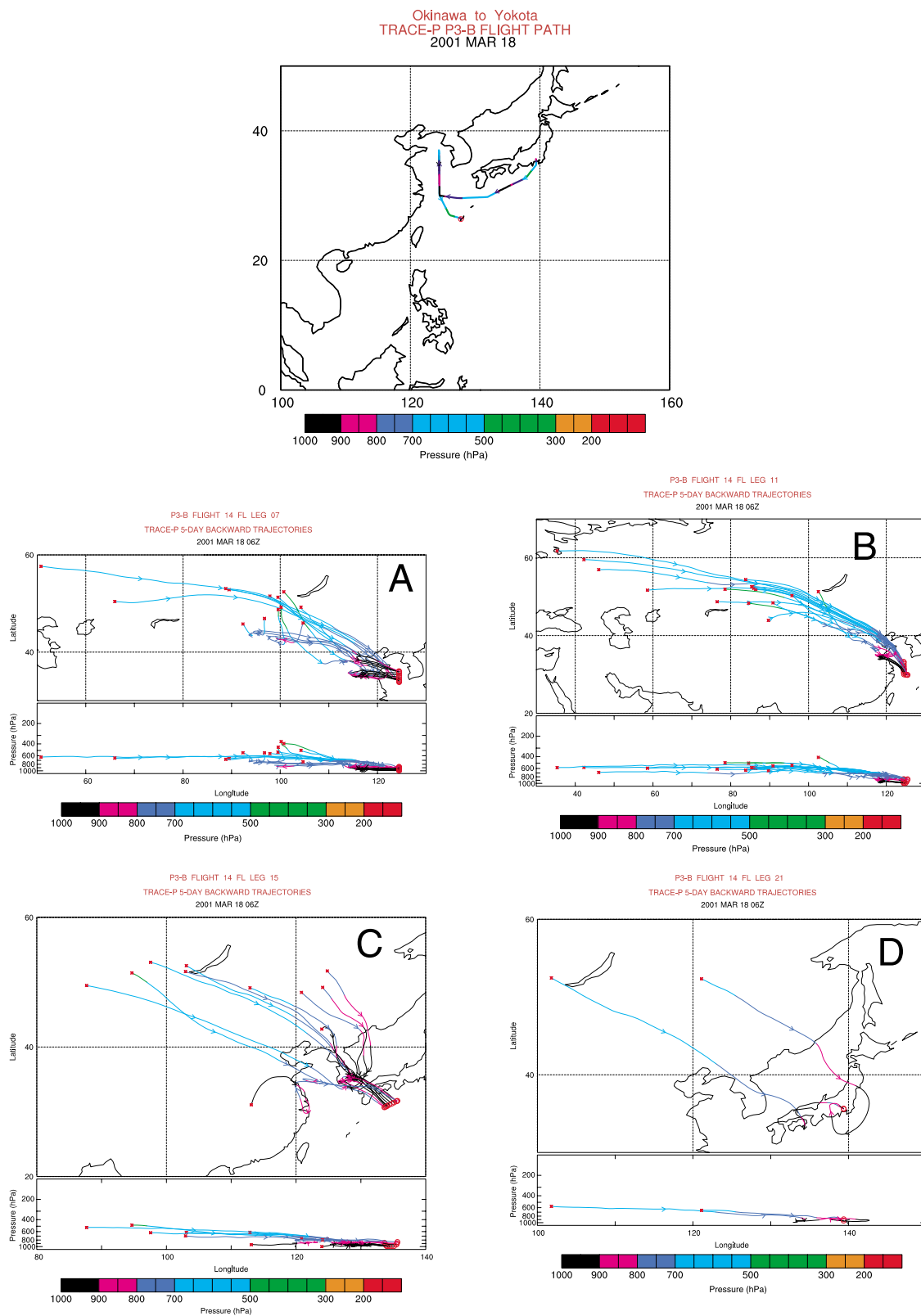
Figure 23. Flight track and backward trajectories for TRACE-P P-3B Flight 14. The different low altitude plumes are marked A–D as in Figure 22.

biomass burning plays a less prominent role, while CO source types that produce relatively low levels of CH_3Br and CH_3Cl are more important for the North China region.

[59] The total emissions of CH_3Br from anthropogenic activities and biomass burning have been estimated to be approximately 74 Gg/yr, with a wide possible range of 44–125 Gg/yr [*WMO*, 2002]. Therefore East Asian emissions of CH_3Br of about 4.7 Gg/yr (from the regions illustrated in Figure 20) would represent approximately 6% of this total. Similarly, total East Asian emissions of CH_3Cl of about 167 Gg/yr (Table 3) represent about 16% of the approximately 1060 Gg/yr emitted globally from biomass burning and industrial activities such as coal combustion [*WMO*, 2002].

3.4.2.3. Halon-1211 and Other Long-Lived Halogenated Gases

[60] Only the South China region subset of data exhibited Halon-1211 mixing ratios that were correlated with CO and were elevated compared to a SE Asian "background" (Figure 21). Comparison with the CO emissions inventory produces an estimate for Halon-1211 emissions from this region of approximately 2.3 Gg/yr (Table 3). For comparison, an increase in the tropospheric burden at its current rate of about 0.1 pptv/yr would require global emissions of about 10 Gg/yr sustained over the 16-year lifetime of Halon-1211 [*WMO*, 2002]. Therefore South China appears to have been a major contributor to the global budget for this gas during the TRACE-P period.

[61] *Palmer et al.* [2003b] quantified Eastern Asian emissions of the halocarbons CCl_4, CH_3CCl_3, CFC-11, and CFC-12 employing the TRACE-P data. They found that the eastern Asian source of CCl_4 was larger than previous estimates and made a significant contribution to global emissions. Emission estimates for CH_3CCl_3, were in general agreement with emission inventory records of production and consumption, but estimates for CFC-11 and CFC-12 estimates were higher than expected.

3.5. Tracers of Asian Outflow: Plumes
3.5.1. P-3B Flight 14: Coastal "Chinese" and "Japanese" Plumes

[62] P-3B Flight 14 was flown from Okinawa to Yokota with a northwards excursion over the Yellow Sea on 18 March 2001 (Figure 22). Several plumes were encountered during the three low altitude legs labeled A, B (representing the "China" category of the Figure 19 correlation plots), and C (representing the "Japan" category). Plume D represents landing in Yokota. The backward trajectories for these plumes are shown in Figure 23.

[63] Plume A was sampled over the Yellow Sea and contained only small enhancements of C_2Cl_4 and CH_3Br, but high levels of biomass burning/biofuel (and possibly coal) combustion tracers consistent with trajectory A showing outflow from China (Figure 23).

[64] Plume B also included outflow from China over the Yellow Sea and contained a similar trace gas signature to Plume A, except that Halon-1211 was very much more elevated than in Plume A. Halon-1211 levels may be more variable than for other gases because large sources (such as a factory still manufacturing the gas) would not be as well dispersed as the smaller point sources of other gases, for example, associated with domestic activities.
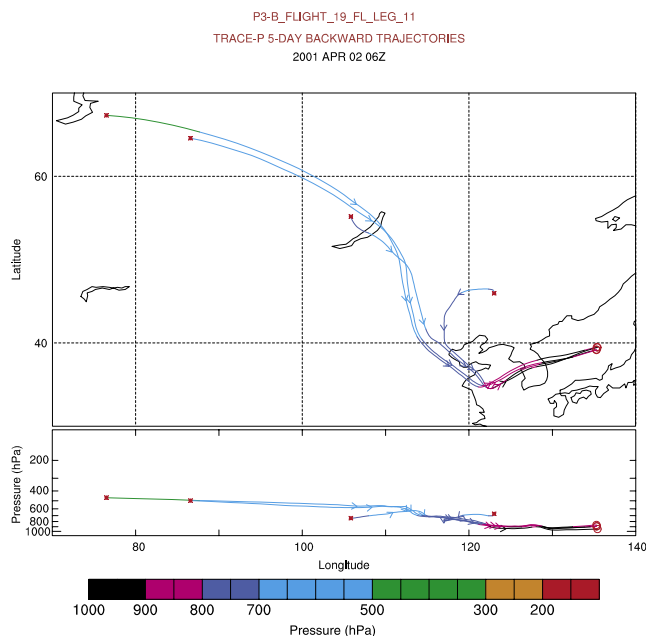
Figure 24. Backward trajectory for a low altitude air mass containing methyl bromide mixing ratios of nearly 35 pptv encountered during TRACE-P P-3B Flight 19, which was a Yokota local flight over the Sea of Japan.

[65] Plume C, sampled over the Pacific off the SE coast of Japan, was characterized by very high levels of methyl bromide (more than 25 pptv). The industrial tracer C_2Cl_4 was also enhanced, as was CH_3CCl_3 (to 59 pptv, not shown), but levels of Halon-1211, ethyne and CH_3Cl were relatively low (Figure 22). Interestingly, the backward trajectories follow a low-altitude path over southern Japan, South Korea and into the vicinity of Seoul approximately 2 days prior to sampling (Figure 23). Landing in Yokota (within the Tokyo air-shed) revealed similarly high CH_3Br and C_2Cl_4 mixing ratios (Figure 22, Plume D).

[66] In addition, very high mixing ratios of CH_3Br (nearly 35 pptv) were observed during P-3B Flight 19, which was a Yokota local flight over the Sea of Japan. The backward trajectories again passed over S Korea and specifically the Seoul region at low altitude less than one day prior to being sampled (Figure 24).

3.5.2. A Case Study of DC-8 Flight 5

[67] Flight 5 was a transit from Kona to Guam flown on 27 February 2001. Various different trace gas signatures were encountered in the plumes labeled as A, B, and C in Figure 25. The first (Plume A) was sampled between about 2 and 4 km altitude just after an excursion to the marine boundary layer (MBL), which was quite clean. Mixing ratios of all four tracers shown in the figure were high in this plume, and it contained the highest levels of the industrial tracers Halon-1211 and C_2Cl_4 for the entire flight. However the combustion tracers CH_3Cl and ethyne were also elevated. Consistent with this, the 5-day backward trajectories originate over industrial regions of southern China where biofuel use is also widespread. Some trajectories also extend to parts of SE Asia where biomass burning was common during the TRACE-P period. Thus Plume A appears to have a mixed biomass/biofuel and industrial origin.
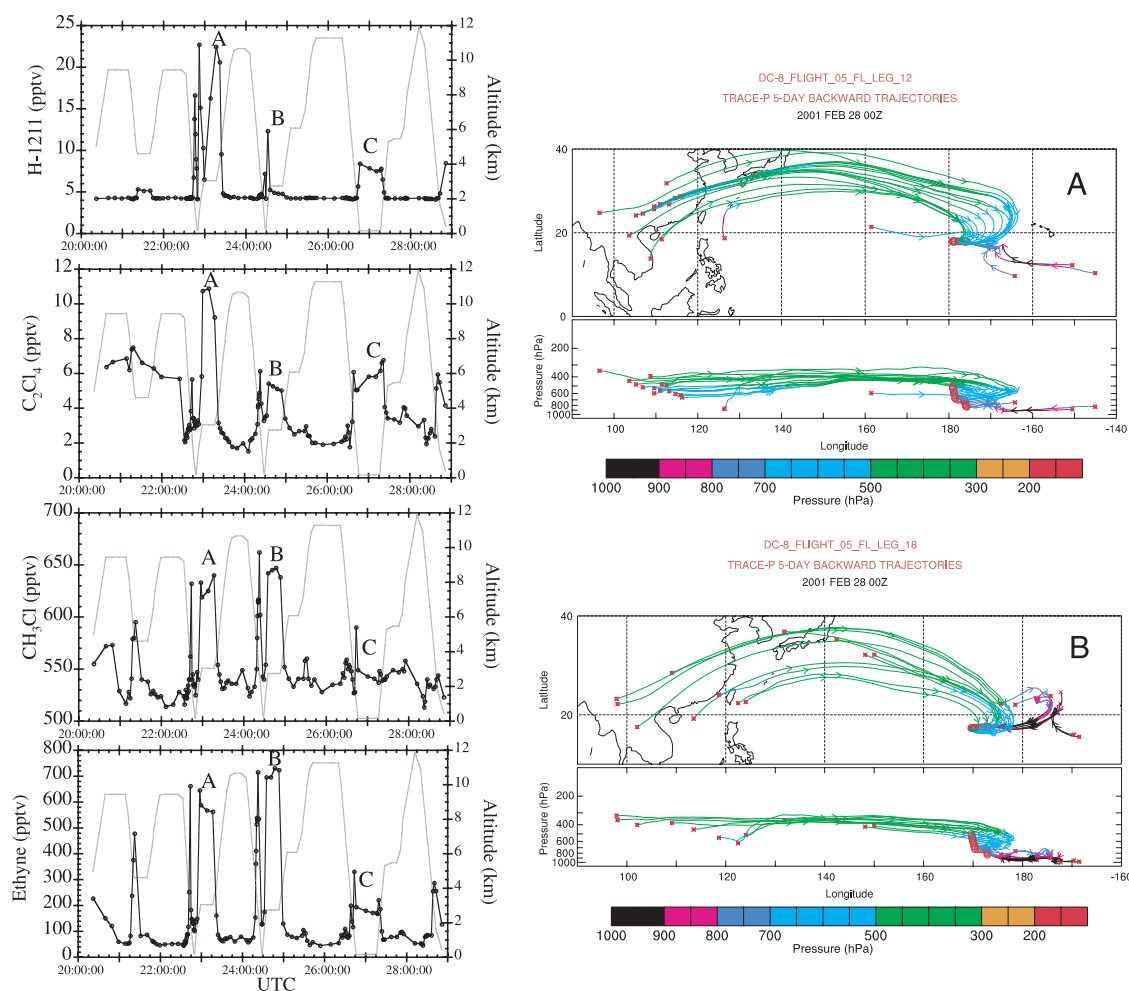
Figure 25. Mixing ratios of selected trace gases and altitude versus time for TRACE-P DC-8 Flight 5. Very high Halon-1211 was observed in plume A, which had a backward trajectory from mixed regions of China. Lower Halon-1211 mixing ratios were observed in plume B, with its backward trajectory potentially showing a greater biomass burning influence from further west.

[68] Plume B, sampled over the same altitude range as Plume A, contained very similar levels of CH_3Cl and ethyne compared to Plume A, indicating a probable biomass burning/biofuel emission component, but levels of C_2Cl_4, and particularly Halon-1211, were much lower than in Plume A. The backward trajectories are very similar but consistent with the different trace gas signatures, the trajectories associated with Plume B have a stronger bias towards an origin over Taiwan and the biomass burning regions of SE Asia, rather than continental China. Being a more developed region, Taiwan would be expected to emit less Halon-1211, but would still emit C_2Cl_4. Thus, combined trace gas signature information and trajectories are needed to conclude that this plume had somewhat different origins than Plume A.

[69] Plume C was sampled closer to but still to the east of Guam. Levels of all the gases are quite low but are still elevated above background, with the exception of CH_3Cl. The fact that C_2Cl_4, H-1211, and ethyne are somewhat elevated is consistent with an aged northern Chinese plume. The 5-day backward trajectories remain over the ocean so do not go back far enough to indicate any particular

continental origin for this air mass, which reinforces the observation that it is well aged.

[70] It does not appear that the large-scale distributions of CH_3Cl provide any evidence for an influence from biomass combustion that can be separated from the general urban biofuel emissions in the regions sampled by the DC-8 and the P-3B.

3.5.3. Biomass Burning Plumes

[71] As mentioned in section 3.2, a notable exception to the general trend of low ethene over the remote Pacific was a plume of pollution in the mid-troposphere that also contained high mixing ratios of ethyne and CH_3Cl, to the NE of the Hawaiian Islands (Figures 2–4). These enhancements were observed during DC-8 transit Flight 4 (Dryden to Kona). One particular vertical profile, centered at approximately 33°N, 210°E, captures the vertical structure of this plume (which was encountered during several ascent/ descents) very well (Figure 26). Between the altitudes of about 6–10 km this plume also contained enhanced ozone (to more than 80 ppbv) but not the industrial tracer C_2Cl_4 (Figure 26), a signature that is indicative of a biomass burning source. The backward trajectories for this vertical
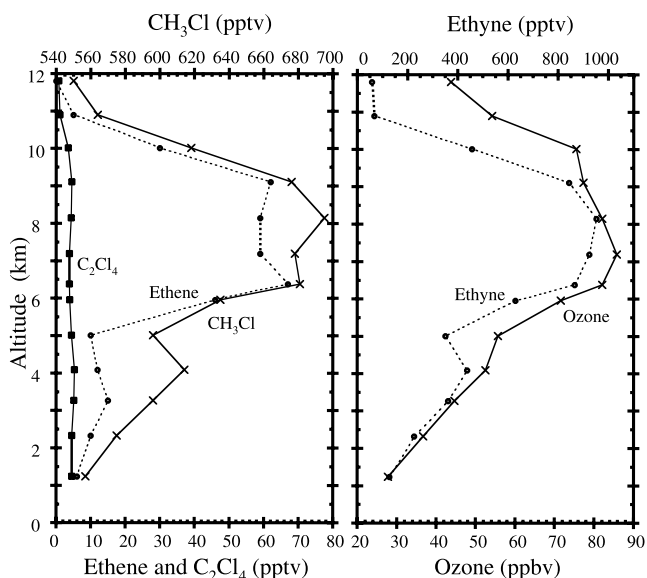
Figure 26. Vertical profile from TRACE-P DC-8 Flight 4, a biomass burning plume in the mid troposphere NE of the Hawaiian Islands.

profile reveal that the polluted air originated at low altitude over Myanmar (Burma) and northern India approximately 5 days previously (Figure 27), regions that *Heald et al.* [2003] have characterized as the sites for many biomass fires throughout the TRACE-P period. This plume is also associated strongly with both fine and coarse aerosols (not shown) indicating that the fire emissions were lifted into the upper free troposphere by a process other than wet convection (possibly frontal lifting [*Liu et al.*, 2003]). *Singh et al.* [2003] suggest that hydrogen cyanide (HCN) and acetonitrile (CH₃CN) may be unique tracers for biomass burning. Indeed, CH₃CN and HCN levels were approxi-

mately doubled over background in this plume [*Singh et al.*, 2003].

[72] The high ozone, CH₃Cl, and ethyne mixing ratios, together with the low background C_2Cl_4 values associated with the Flight 4 plume, are reminiscent of the many biomass burning plumes that were encountered at similar altitudes over the south Pacific during PEM-Tropics A [*Blake et al.*, 1999]. However, these latter plumes had backward trajectories linking them with emissions from southern Africa and Brazil 10 days or so previously, and unlike this relatively fresh TRACE-P plume, the ethene levels had long decayed to background before sampling.

4. Conclusions

[73] Trace gas signatures combined with backward trajectories illustrated that during TRACE-P the western Pacific was influenced by a wide variety of sources, including emissions from vehicle/biofuel/coal/biomass combustion and industrial activities. Asian continental outflow tended to contain a mixture of emissions that often made it difficult to pinpoint the influence of specific sources or regions.

[74] There were remarkably few changes in levels of the NMHCs and CO during the 7-year period between 1994 PEM-West B and 2001 TRACE P, in spite of projected NMHC increases. The significant decreases in mixing ratios of the short-lived NMHCs that instead were observed at the highest sampled latitudes were attributed to the 3-week seasonal offset between the periods covered by the two campaigns. The comparable CH₃Cl levels observed for both PEM-West B and TRACE-P are consistent with biomass burning and biofuel use remaining relatively stable over this time period. Levels of bromine-containing Halon-1211 increased by about 50% from 1994 to 2001. As in previous airborne measurement campaigns, CH₃Cl and Halon-1211 proved to be useful markers for air masses of southern
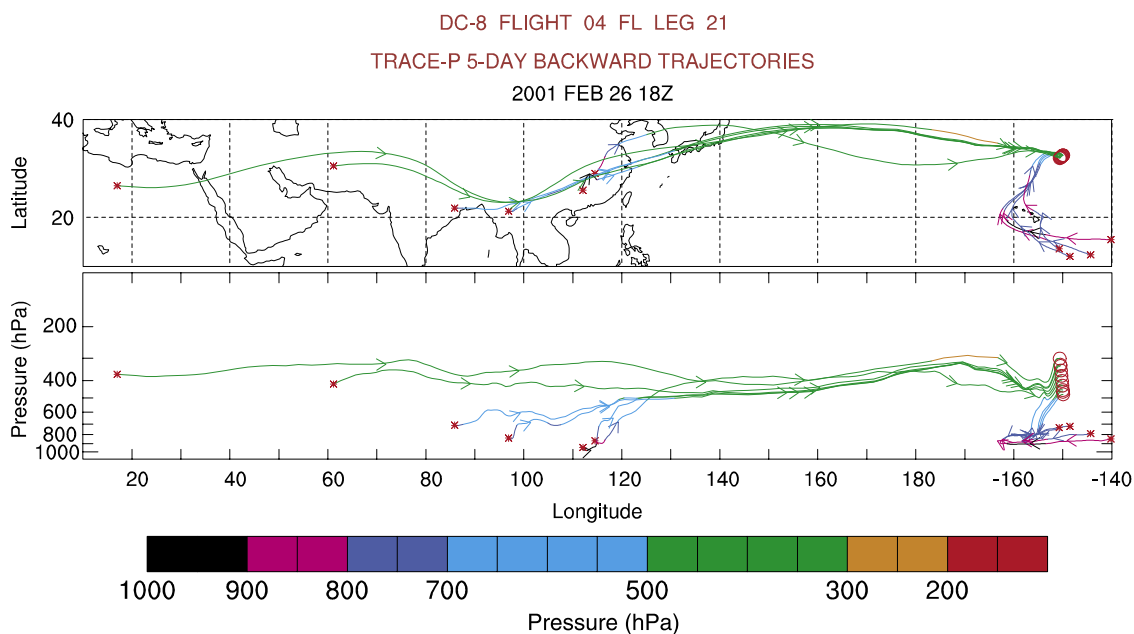

Figure 27. Backward trajectories for the vertical profile in Figure 26.

Chinese origin. The results presented here support the finding that southern China is a substantial source of Halon-1211.

[75] Mixing ratios of CH_3CCl_3, CCl_4 and C_2Cl_4 were significantly lower during TRACE-P compared to PEM-West B. In accord with Montreal Protocol regulations, TRACE-P levels of CH_3CCl_3 were only 1/3 of those measured in 1994. Hot spots of CCl_4 and CH_3CCl_3 were observed in Chinese outflow. Methyl chloroform was also elevated in air associated with regions of Japan and Korea, indicating additional remaining CH_3CCl_3 sources.

[76] Methyl bromide levels decreased by nearly 20% (2.1 ± 0.9 pptv for 0–2 km) in the period between PEM-West B and TRACE-P. However, elevated mixing ratios of CH_3Br were frequently observed during TRACE-P in air masses that had been advected over Japanese and Korean Ports. Therefore these enhancements were possibly associated with the use of CH_3Br as an import/export crop fumigant, which is exempt from the Montreal Protocol. As a consequence, emissions of CH_3Br from Japan and Korea were estimated to be almost as large as for all of South China. Total East Asian emissions of CH_3Br and CH_3Cl were estimated to be about 4.7 Gg/yr and 167 Gg/yr, respectively, in 2001.

References

Anderson, J., J. M. Russel III, S. Solomon, and L. E. Deaver, Halogen Occultation Experiment confirmation of stratospheric chlorine decreases in accordance with the Montreal Protocol, *J. Geophys. Res.*, *105*, 4483–4490, 2000.

Andreae, M. O., E. Atlas, H. Cachier, W. R. Cofer III, G. W. Harris, G. Helas, R. Koppmann, J.-P. Lacaux, and D. E. Ward, Trace gas and aerosol emissions from savanna fires, in *Biomass Burning and Global Change*, vol. 1, edited by J. S. Levine, pp. 278–295, MIT Press, Cambridge, Mass., 1996.

Apel, E. C., J. G. Calvert, and F. C. Fehsenfeld, The Nonmethane Hydrocarbon Intercomparison Experiment (NOMHICE): Tasks 1 and 2, *J. Geophys. Res.*, *99*, 16,651–16,664, 1994.

Apel, E. C., J. G. Calvert, T. M. Gilpin, and F. C. Fehsenfeld, The Nonmethane Hydrocarbon Intercomparison Experiment (NOMHICE): Task 3, *J. Geophys. Res.*, *104*, 26,069–26,086, 1999.

Bey, I., D. J. Jacob, J. A. Logan, and R. M. Yantosca, Asian chemical outflow to the Pacific: Origins, pathways and budgets, *J. Geophys. Res.*, *106*, 23,097–23,114, 2001.

Blake, D. R., and F. S. Rowland, Global atmospheric concentrations and source strengths of ethane, *Nature*, *321*, 231–233, 1986.

Blake, D. R., and F. S. Rowland, Urban leakage of liquefied petroleum gas and its impact on Mexico City air quality, *Science*, *269*, 953–956, 1995.

Blake, D. R., D. F. Hurst, T. W. Smith Jr., W. J. Whipple, T.-Y. Chen, N. J. Blake, and F. S. Rowland, Summertime measurements of selected nonmethane hydrocarbons in the Arctic and subarctic during the 1988 Arctic Boundary Layer Expedition (ABLE-3A), *J. Geophys. Res.*, *97*, 16,559–16,588, 1992.

Blake, D. R., T. Y. Chen, T. W. Smith Jr., C. J.-L. Wang, O. W. Wingenter, N. J. Blake, F. S. Rowland, and E. W. Mayer, Three-dimensional distribution of NMHCs and halocarbons over the northwestern Pacific during the 1991 Pacific Exploratory Mission (PEM-West A), *J. Geophys. Res.*, *101*, 1763–1778, 1996.

Blake, N. J., D. R. Blake, B. C. Sive, T.-Y. Chen, J. E. Collins Jr., G. W. Sachse, B. E. Anderson, and F. S. Rowland, Biomass burning emissions and vertical distribution of atmospheric methyl halides and other reduced carbon gases in the South Atlantic Region, *J. Geophys. Res.*, *101*, 24,151–24,164, 1996.

Blake, N. J., D. R. Blake, T.-Y. Chen, J. E. Collins Jr., G. W. Sachse, B. E. Anderson, and F. S. Rowland, Distribution and seasonality of selected hydrocarbons and halocarbons over the western Pacific basin during PEM-West A and PEM-West B, *J. Geophys. Res.*, *102*, 28,315–28,331, 1997.

Blake, N. J., et al., Influence of southern hemispheric biomass burning on mid-tropospheric distributions of nonmethane hydrocarbons and selected halocarbons over the remote South Pacific, *J. Geophys. Res.*, *104*, 16,213–16,232, 1999.

Blake, N. J., et al., Large-scale latitudinal and vertical distributions of NMHCs and selected halocarbons in the troposphere over the Pacific Ocean during the March–April 1999 Pacific Exploratory Mission (PEM-Tropics B), *J. Geophys. Res.*, *106*, 32,627–32,644, 2001.

Blake, N. J., D. R. Blake, B. C. Sive, A. S. Katzenstein, S. Meinardi, O. W. Wingenter, E. L. Atlas, F. Flocke, B. A. Ridley, and F. S. Rowland, The seasonal evolution of NMHCs and light alkyl nitrates at mid to high northern latitudes during TOPSE, *J. Geophys. Res.*, *108*(D4), 8359, doi:10.1029/2001JD001467, 2003.

Butler, J. H., Better budgets for methyl halides?, *Nature*, *403*, 260–261, 2000.

Butler, J. H., S. A. Montzka, A. D. Clarke, J. M. Lobers, and J. W. Elkins, Growth and distribution of halons in the atmosphere, *J. Geophys. Res.*, *103*, 1503–1511, 1998.

Carmichael, G. R., et al., Evaluating regional emission estimates using the TRACE-P Observations, *J. Geophys. Res.*, *108*(D21), 8823, doi:10.1029/2002JD003116, in press, 2003.

Colman, J. J., A. L. Swanson, S. Meinardi, B. C. Sive, D. R. Blake, and F. S. Rowland, Description of the analysis of a wide range of volatile organic compounds in whole air samples collected during PEM-Tropics A and B, *Anal. Chem.*, *73*, 3723–3731, 2001.

Davis, D. D., et al., Trends in western North Pacific ozone photochemistry as defined by observations from NASA's PEM-WEST B (1994) and TRACE-P (2001) field studies, *J. Geophys. Res.*, *108*, doi:10.1029/2002JD003232, in press, 2003.

Ehhalt, D. H., F. Rohrer, A. B. Knaus, M. J. Prather, D. R. Blake, and F. S. Rowland, On the significance of regional trace gas distributions as derived from aircraft campaigns in PEM-West A and B, *J. Geophys. Res.*, *102*, 28,333–28,351, 1997.

Engel, A., U. Schmidt, and D. Mckenna, Stratospheric trends of CFC-12 over the past two decades: Recent observational evidence of declining growth rates, *Geophys. Res. Lett.*, *25*, 3319–3322, 1998.

Fraser, P. J., D. E. Oram, C. E. Reeves, S. A. Penkett, and A. McCulloch, Southern Hemispheric halon trends (1978–1998) and global halon emissions, *J. Geophys. Res.*, *104*(D13), 15,985–16,000, 1999.

Fuelberg, H. E., C. M. Kiley, J. R. Hannan, D. J. Westberg, M. A. Avery, and R. E. Newell, Atmospheric transport during the Transport and Chemical Evolution over the Pacific (TRACE-P) experiment, *J. Geophys. Res.*, *108*(D20), 8782, doi:10.1029/2002JD003092, in press, 2003.

Gupta, M. L., R. J. Cicerone, D. R. Blake, F. S. Rowland, and I. S. A. Isaksen, Global atmospheric concentrations and source strengths of light hydrocarbons and tetrachloroethene, *J. Geophys. Res.*, *103*, 28,219–28,235, 1998.

Heald, C., et al., Biomass burning emission inventory with daily resolution: Application to aircraft observations of Asian outflow, *J. Geophys. Res.*, *108*(D21), 8811, doi:10.1029/2002JD003082, in press, 2003.

Hoell, J. M., D. D. Davis, S. C. Liu, R. E. Newell, H. Akimoto, R. J. McNeal, and R. J. Bendura, The Pacific Exploratory Mission-West Phase B: February–March, 1994, *J. Geophys. Res.*, *102*, 28,223–28,239, 1997.

Jacob, D. J., J. H. Crawford, M. M. Kleb, V. E. Connors, R. J. Bendura, and J. L. Raper, The Transport and Chemical Evolution over the Pacific (TRACE-P) mission: Design, execution, and first results, *J. Geophys. Res.*, *108*(D20), 8781, doi:10.1029/2002JD003276, in press, 2003.

Johnston, N. A. C., J. J. Colman, D. R. Blake, M. J. Prather, and F. S. Rowland, On the variability of tropospheric gases: Sampling, loss patterns, and lifetime, *J. Geophys. Res.*, *107*(D11), 4111, doi:10.1029/2001JD000669, 2002.

Jordan, C. E., et al., Chemical and physical properties of bulk aerosols within four sectors observed during TRACE-P, *J. Geophys. Res.*, *108*(D21), 8817, doi:10.1029/2002JD003101, in press, 2003.

Kato, N., An analysis of the structure of energy consumption and dynamics of emissions of atmospheric species related to the global environmental change (SO_2, NO_x, and CO_2), *Atmos. Environ.*, *30*, 757–785, 1996.

Kita, K., et al., Sources, distribution and partitioning of reactive nitrogen in the lower troposphere over western Pacific during TRACE-P, *Eos Trans. AGU*, *83*(47), Fall Meet. Suppl., Abstract A62A-0134, 2002.

Liu, H., D. J. Jacob, I. Bey, R. M. Yantosca, B. N. Duncan, and G. W. Sachse, Transport pathways for Asian combustion outflow over the Pacific: Interannual and seasonal variations, *J. Geophys. Res.*, *108*(D20), 8786, doi:10.1029/2002JD003102, in press, 2003.

Martin, B., H. Fuelberg, N. Blake, D. Blake, J. Crawford, and J. Logan, Long range transport of Asian outflow to the Equatorial Pacific, *J. Geophys. Res.*, *108*(D2), 8233, doi:10.1029/2001JD001418, 2002.

Merrill, J. T., R. E. Newell, and A. S. Bachmeier, A meteorological overview for the Pacific Exploratory Mission-West Phase B, *J. Geophys. Res.*, *102*, 28,241–28,253, 1997.

Montzka, S. A., J. H. Butler, J. W. Elkins, T. M. Thompson, A. D. Clarke, and L. T. Lock, Present and future trends in the atmospheric burden of ozone-depleting halogens, *Nature*, *398*, 690–693, 1999.

Montzka, S. A., J. Lind, J. H. Butler, B. Hall, D. Mondeel, and J. W. Elkins, Recent declines in atmospheric methyl bromide from a global flask sampling network, *Eos Trans. AGU*, *83*(47), Fall Meet. Suppl., Abstract A72C-0184, 2002.

Palmer, P. I., D. J. Jacob, D. B. A. Jones, C. I. Heald, R. M. Yantosca, J. A. Logan, G. W. Sachse, and D. G. Streets, Inverting for emissions of carbon monoxide from Asia using aircraft observations over the western Pacific, *J. Geophys. Res.*, *108*(D21), 8828, doi:10.1029/2003JD003397, in press, 2003a.

Palmer, P. I., D. J. Jacob, L. J. Mickley, D. R. Blake, G. W. Sachse, H. E. Fuelberg, and C. M. Kiley, Eastern Asian emissions of anthropogenic halocarbons deduced from aircraft concentration data, *J. Geophys. Res.*, 108, doi:10.1029/2003JD003591, in press, 2003b.

Penkett, S. A., N. J. Blake, P. Lightman, A. R. W. Marsh, P. Anwyl, and G. Butcher, The seasonal variation of non-methane hydrocarbons in the free troposphere over the North Atlantic Ocean: Possible evidence for extensive reaction of hydrocarbons with the nitrate radical, *J. Geophys. Res.*, *98*, 2865–2885, 1993.

Prinn, R. G., R. F. Weiss, B. R. Miller, J. Huang, F. N. Alyea, D. M. Cunnold, P. J. Fraser, D. E. Hartley, and P. G. Simmonds, Atmospheric trend and lifetime of CH_3CCl_3 and global OH concentrations, *Science*, *269*, 187–192, 1995.

Prinn, R. G., et al., A history of chemically and radiatively important gases in air deduced from ALE/GAGE/AGAGE, *J. Geophys. Res.*, *105*, 17,751–17,792, 2000.

Prinn, R. G., et al., Evidence for substantial variations of atmospheric hydroxyl radicals in the past two decades, *Science*, *292*, 1882–1888, 2001.

Rasmussen, R. A., L. E. Rasmussen, M. A. K. Khalil, and R. W. Dalluge, Concentration and distribution of methyl chloride in the atmosphere, *J. Geophys. Res.*, *85*, 7350–7356, 1980.

Rasmussen, R. A., M. A. K. Khalil, and J. S. Chang, Atmospheric trace gases over China, *Environ. Sci. Technol.*, *16*, 124–126, 1982.

Romashkin, P. A., D. F. Hurst, J. W. Elkins, G. S. Dutton, and P. R. Wamsley, Effect of the tropospheric trend on the stratospheric tracer-tracer correlations: Methyl chloroform, *J. Geophys. Res.*, *104*, 26,643–26,652, 1999.

Rudolph, J., The tropospheric distribution and budget of ethane, *J. Geophys. Res.*, *100*, 11,369–11,381, 1995.

Russo, R., et al., Chemical composition of Asian outflow over the western Pacific: Results from TRACE-P, *J. Geophys. Res.*, *108*(D20), 8804, doi:10.1029/2002JD003184, in press, 2003.

Seinfeld, J. H., and S. N. Pandis, *Atmospheric Chemistry and Physics*, John Wiley, New York, 1998.

Shirai, T., and Y. Makide, Rapidly increasing concentrations of CFC alternatives (HFC-134a, HCFC-141b, and HCFC-142b) in the atmosphere as observed in Hokkaido and Antarctica, *Chem. Lett.*, *4*, 357–358, 1998.

Simmonds, P. G., D. M. Cunnold, R. F. Weiss, R. G. Prinn, P. J. Fraser, A. McCulloch, F. N. Alyea, and S. O'Doherty, Global trends and emission estimates of CCl_4 from in situ background observations from July 1978 to June 1996, *J. Geophys. Res.*, *103*, 16,017–16,027, 1998.

Simpson, I. J., N. J. Blake, E. Atlas, F. Flocke, J. H. Crawford, H. E. Fuelberg, C. M. Kiley, F. S. Rowland, and D. R. Blake, Photochemical production of selected C_2-C_5 alkyl nitrates in tropospheric air influenced by Asian outflow, *J. Geophys. Res.*, *108*(D20), 8808, doi:10.1029/2002JD002830, in press, 2003.

Singh, H. B., et al., In situ measurements of HCN and CH_3CN in the Pacific troposphere: Sources, sinks, and intercomparisons with spectroscopic observations, *J. Geophys. Res.*, *108*(D20), 8795, doi:10.1029/2002JD003006, in press, 2003.

Sive, B. C., Analytical methods and estimated hydroxyl radical concentrations, Ph.D. thesis, Univ. of Calif., Irvine, Irvine, Calif., 1998.

Smyth, S., et al., Comparison of free tropospheric western Pacific air mass classification schemes for the PEM-West A experiment, *J. Geophys. Res.*, *101*, 1743–1762, 1996.

Streets, D. G., An inventory of gaseous and primary aerosol emissions in Asia in the year 2000, *J. Geophys. Res*, *108*(D21), 8809, doi:10.1029/2001JD001445, 2003.

Swanson, A. L., N. J. Blake, E. Atlas, F. Flocke, D. R. Blake, and F. S. Rowland, Seasonality of C_2-C_4 NMHC and C_1-C_4 alkyl nitrates on the Arctic ice-sheet at Summit, Greenland, *J. Geophys. Res.*, *108*(D2), 4065, doi:10.1029/2001JD001445, 2003.

Talbot, R. W., et al., Chemical characteristics of continental outflow from Asia to the troposphere over the western Pacific Ocean during February–March 1994: Results from PEM-West B, *J. Geophys. Res.*, *102*, 28,255–28,274, 1997.

Talbot, R., et al., Reactive nitrogen in Asian continental outflow over the western Pacific: Results from the NASA TRACE-P airborne mission, *J. Geophys. Res.*, *108*(D20), 8803, doi:10.1029/2002JD003129, in press, 2003.

United Nations Environment Programme (UNEP), *Handbook for the Montreal Protocol on Substances That Deplete the Ozone Layer*, 2nd ed., Ozone Secr., Nairobi, Kenya, 1991.

United Nations Environment Programme (UNEP), *Report of the Halon Fire Extinguishing Agents Technical Options Committee, 1998 Assessment*, Geneva, Switzerland, 1998a.

United Nations Environment Programme (UNEP), *Report of the Methyl Bromide Technical Options Committee, 1998 Assessment of Alternatives to Methyl Bromide*, Geneva, Switzerland, 1998b.

United Nations Environment Programme (UNEP), *Report of the Aerosols, Sterilants, Miscellaneous Uses and Carbon Tetrachloride Technical Options Committee*, Geneva, Switzerland, 1999.

United Nations Environment Programme (UNEP), *Production and Consumption of Ozone Depleting Substances under the Montreal Protocol 1986–2000*, Geneva, Switzerland, 2002.

U.S. Environmental Protection Agency, Chemicals in the environment: Perchloroethylene, *CAS 127-18-4*, Washington, D. C., 1994.

Wang, C. J.-L., Global concentrations of selected halocarbons, 1998–1992, Ph.D. dissertation, Univ. of Calif., Irvine, Irvine, Calif., 1993.

World Meteorological Organization (WMO), Scientific assessment of Ozone Depletion: 1998, Global Ozone Research and Monitoring Project, *Rep. 44*, Geneva, Switzerland, 1999.

World Meteorological Organization/United Nations Environment Programme, *Scientific Assessment of Ozone Depletion: 2002, Global Ozone Research and Monitoring Project*, Geneva, Switzerland, 2002.

Yokouchi, Y., D. Doom-Sauntry, K. Yazawa, T. Inagaki, and T. Tamuru, Recent decline of methyl bromide in the troposphere, *Atmos. Environ.*, *36*, 4985–4989, 2002.

———————

E. Atlas, Atmospheric Chemistry Division, National Center for Atmospheric Research, 1850 Table Mesa Dr., Boulder, CO 80305, USA. (atlas@ucar.edu)

M. Avery, G. Sachse, and S. Vay, NASA Langley Research Center, Hampton, VA 23681, USA. (m.a.avery@larc.nasa.gov; g.w.sachse@larc.nasa.gov; s.a.vay@larc.nasa.gov)

B. Barletta, D. R. Blake, N. J. Blake, A. S. Katzenstein, J. P. Lopez, S. Meinardi, F. S. Rowland, A. L. Swanson, and I. S. Simpson, Department of Chemistry, 516 Rowland Hall, University of California, Irvine, Irvine, CA 92697-2025, USA. (bbarlett@uci.edu; drblake@uci.edu; nblake@uci.edu; akatzens@uci.edu; jlopez@mail.arc.nasa.gov; smeinard@uci.edu; rowland@uci.edu; aswanson@ucar.edu; isimpson@uci.edu)

H. E. Fuelberg and C. M. Kiley, Department of Meteorology, Florida State University, Tallahassee, FL 32306, USA. (fuelberg@huey.met.fsu.edu; ckiley@huey.met.fsu.edu)

K. Kita, Department of Environmental Sciences, Faculty of Science, Ibaraki University, 2-1-1 Bunkyo, Mito, Ibaraki 310-8512, Japan. (kita@mx.ibaraki.ac.jp)

T. Shirai, Earth Observation Research Center, National Space Development Agency of Japan, Harumi Island Triton Square Office Tower X 23 F, 1-8-10 Harumi, Chuo-ku, Tokyo 104-0023, Japan. (shirai@eorc.nasda.go.jp)